Chemical Geology 493 (2018) 136–152

Contents lists available at ScienceDirect

Chemical Geology

journal homepage: www.elsevier.com/locate/chemgeo

Invited Review Article

Oscillating redox conditions in the Vocontian Basin (SE France) during Oceanic Anoxic Event 2 (OAE 2)

Julien Danzelle[a,*], Laurent Riquier[a], François Baudin[a], Christophe Thomazo[b], Emmanuelle Pucéat[b]

[a] Sorbonne Université, CNRS-INSU, ISTeP UMR 7193, 4 Place Jussieu, 75005 Paris, France
[b] Université Bourgogne Franche-Comté, Biogéosciences UMR CNRS 6282, 6 Bd Gabriel, 21000 Dijon, France

ARTICLE INFO

Editor: Michael E. Böttcher

Keywords:
OAE 2
Vocontian Basin
Redox conditions
Trace metals
Iron speciation
Sulfur isotope

ABSTRACT

The Cenomanian-Turonian boundary (~94 Ma) was marked by an episode of widespread organic carbon burial largely associated with low oxygen concentrations in bottom oceanic waters, named Oceanic Anoxic Event 2 (OAE 2). In the Vocontian Basin (SE France), the Pont d'Issole section exposes a 22 m interval called Niveau Thomel, the local sedimentary expression of the OAE 2, characterized by levels of laminated dark shales with marine-derived organic matter enrichments (up to 2.5 wt%). An episodic disruption in total organic carbon (TOC) enrichment is observed in bioturbated limestones within the Niveau Thomel, reflecting bottom-water reoxygenation associated to the Plenus Cold Event. Oscillations in redox conditions during the OAE 2 are evidenced by variations in the degree of pyritisation of the sediments reflecting suboxic to anoxic conditions associated with organic-rich intervals. These variations are additionally highlighted by enrichments in redox-sensitive trace elements (Mo, V, Zn) in sediments containing at least 1.5 wt% TOC, which may reflect a threshold between suboxic and anoxic conditions at Pont d'Issole section. Low Mn and Fe concentrations in > 0.3 wt% TOC samples mark a large O_2 depletion in pore waters. Phosphorus released from the sediments under deoxygenated conditions could have contributed to sustain the primary productivity in the basin, promoting further O_2 consumption. A large negative excursion in the sulfur isotopic composition of pyrite ($\delta^{34}S_{py}$) with minimum values down to −40‰ suggests that microbial sulfate reduction was non sulfate-limited and was characterized by pyrite precipitation in an open system with regard to the marine sulfate reservoir. This feature is probably linked to a higher sulfate availability within the Vocontian Basin due to important Large Igneous Province outgassing at the onset of the OAE 2.

1. Introduction

The Cretaceous was a period marked by the occurrence of Oceanic Anoxic Events (Jenkyns, 2010) evidenced by enhanced accumulation of organic matter in the sediments. The Oceanic Anoxic Event 2 (OAE 2), spanning the Cenomanian-Turonian boundary (CTB; ~94 Ma), represents the most expanded OAE with widespread synchronous deposition of organic-rich sediments, referred as black shales (Schlanger and Jenkyns, 1976; Jenkyns, 1980; Arthur et al., 1990) (Fig. 1). Massive burial of isotopically light organic carbon is reflected by a > 2‰ positive excursion in the global carbon isotopic signature of carbonates and organic matter during this event (Scholle and Arthur, 1980; Tsikos et al., 2004). It has been suggested that the main driver of this evolution was the development of worldwide basin bottom-water anoxia due to a conjuncture of favorable conditions (Meyer and Kump, 2008). In the Cenomanian-Turonian time interval, an extremely warm climate (Pucéat et al., 2003; Forster et al., 2007; Friedrich et al., 2012. O'Brien et al., 2017) and the resulting reduced latitudinal thermal gradient limited oxygen solubility in the oceans (Hotinski et al., 2001; Takashima et al., 2006). This was probably favored by high atmospheric CO_2 concentrations and favorable paleogeography (Barron et al., 1995; Royer et al., 2012). Emplacement of Large Igneous Provinces (LIPs; Fig. 1) at that time, like the Caribbean LIP and High Arctic LIP (Snow et al., 2005; Kuroda et al., 2007; Turgeon and Creaser, 2008; Du Vivier et al., 2014) is usually considered to be the source of increased oceanic and atmospheric CO_2 concentrations (Sinninghe Damsté et al., 2008). Strong temporal correlation between OAEs occurrence and LIPs emplacements (Jones and Jenkyns, 2001) is consistent with this inference.

As a consequence, a blooming primary productivity that thrive on

* Corresponding author at: Sorbonne Université, Campus Pierre et Marie Curie, UMR ISTeP, Case 117, 4 place Jussieu, 75005 Paris, France.
E-mail address: julien.danzelle@upmc.fr (J. Danzelle).

https://doi.org/10.1016/j.chemgeo.2018.05.039
Received 24 January 2018; Received in revised form 22 May 2018; Accepted 25 May 2018
Available online 28 May 2018
0009-2541/

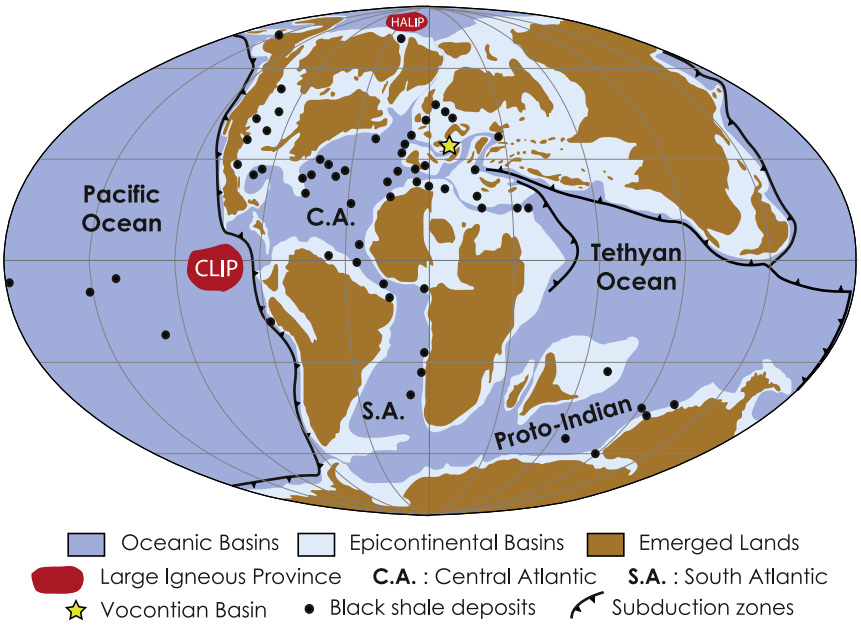

Fig. 1. Global distribution of black shale deposits and major Large Igneous Provinces (LIPs), the Caribbean LIP (CLIP) and High Arctic LIP (HALIP), associated with Cenomanian-Turonian boundary. Black circles represent the location of the black shales compiled from the literature (modified from the compilations published in Takashima et al., 2006 and Trabucho Alexandre et al., 2010). Paleogeographic reconstruction was modified from Blakey (2011).

newly available micronutrients such as reduced metals may have contributed to marine dissolved depletion through enhanced export of organic matter and its oxidation to deplete marine dissolved oxygen (Sinton and Duncan, 1997; Leckie et al., 2002; Monteiro et al., 2012). An accelerated hydrological cycle and enhanced silicate weathering could also have contributed to increased nutrient input to the oceans (Mort et al., 2007a; Frijia and Parente, 2008; Pogge von Strandmann et al., 2013). Regional parameters such as basin spatial configurations and associated oceanic circulation dynamics might account for the worldwide variations in the expression of the OAE 2 in terms of intensity and kinetic parameters (Trabucho Alexandre et al., 2010; van Helmond et al., 2014; Zheng et al., 2016). For instance, deep and confined oceanic basins, as the Central Atlantic at that time, appear prone to sluggish deep circulation, pronounced stratification and intense anoxic conditions (van Helmond et al., 2014; Donnadieu et al., 2016).

Presence of organic-rich sediments in the deepest parts of the Vocontian Basin (SE France) indicates that O_2-depleted conditions in bottom waters during the OAE 2 reached this epicontinental setting. Alternation between laminated dark shales with TOC values up to 2.5 wt% and bioturbated carbonates reveals, however, important variations in the sedimentary regime and redox conditions (Crumière et al., 1990; Jarvis et al., 2011). An important phase of disturbance within the dark shale interval has been attributed to a cooling episode within the OAE 2, called the Plenus Cold Event (PCE), evidenced by a transient return toward lighter values in the $\delta^{13}C$ record within the positive excursion (Jarvis et al., 2011). This episode, recognized in several Central Atlantic and Tethyan sites corresponds to a spreading of cooler waters southward and is interpreted as a negative climatic feedback response after organic carbon sequestration and subsequent drop in atmospheric pCO_2 (Jarvis et al., 2011).

To precisely assess temporal variations in organic burial and redox conditions in the Pont d'Issole section, concentrations of selected redox-sensitive trace elements (RSTE) were measured and iron mineral speciation was performed and was confronted with TOC measurements. Redox facies were attributed following the depositional environments described in Tyson and Pearson (1991) and redefined in Algeo and Maynard (2004) and in Tribovillard et al. (2006). Oxic conditions corresponds to O_2 concentrations in bottom waters > 2.0 $ml{\cdot}l^{-1}$ allowing for aerobic decay of organic matter. Between 2.0 and 0.2 ml $O_2{\cdot}l^{-1}$ H_2O, conditions are referred as suboxic and presence of H_2S is restricted to the pore waters below the sediment-water interface. When free O_2 in bottom waters become strongly depleted, i.e. < 0.2 $ml{\cdot}l^{-1}$ H_2O, conditions are considered as anoxic (non-sulfidic). Anoxic facies may correspond to the expansion of a zone of free H_2S toward the sediment-water interface. Finally, when H_2S reaches the bottom waters and then when O_2 is absent depositional environment is referred to as euxinic (anoxic sulfidic).

We also investigated the evolution of the biogeochemical sulfur cycling and its expression, using $\delta^{34}S$ analyses of extracted pyrite. Sulfur isotope composition, presented here, not only provides new clues on microbial sulfate-reducing (MSR) activity in this basin but also on intra-basin connections between sulfide and sulfate reservoirs and sulfate availability for MSR.

2. Geological setting

Since the early Cretaceous, the Vocontian Basin was an epicontinental gulf forming part of the northern Alpine Ocean in the Tethyan realm at a latitudinal position between 30° and 35°N (Dercourt et al., 1993) (Fig. 2). All along the Late Cretaceous, this basin was affected by a N-S compressive dynamic (Porthault, 1974) linked to the initiation of the closure of the entire Tethys Ocean. These movements were the major agent governing the geometry of several local basins. The Vocontian Basin was bordered to the west by the crystalline Massif Central and in the south by the Durancian isthmus. To the East, the basin seemed less confined even if the deepest domain was structurally disconnected from the submarine platform by active strike-slip faults (Grosheny et al., 2017; Fig. 2). Maximal paleodepths in the Vocontian Basin at the CTB was estimated to few hundred meters based on storm deposits on the outer platform and the presence of sponge spicules reflecting hemipelagic sedimentation (Grosheny et al., 2006). The CTB usually consists of a peculiar facies marked by a distinct interval of dark marls enriched in organic matter content, up to 3% (Crumière et al., 1990; Takashima et al., 2009; Jarvis et al., 2011). This ~20–25 m interval called Niveau Thomel extending to the deepest parts of the basin (Fig. 2) has been related to OAE 2 first because of its organic matter content and its foraminifera biostratigraphy (Crumière, 1989), and is considered as an equivalent to the Bonarelli Level in Umbria-Marche in Italy (Arthur and Premoli Silva, 1982). Its link with the OAE 2 has been further confirmed by the stable carbon isotope signature of both inorganic and organic material (Morel, 1998; Jarvis et al., 2011), which

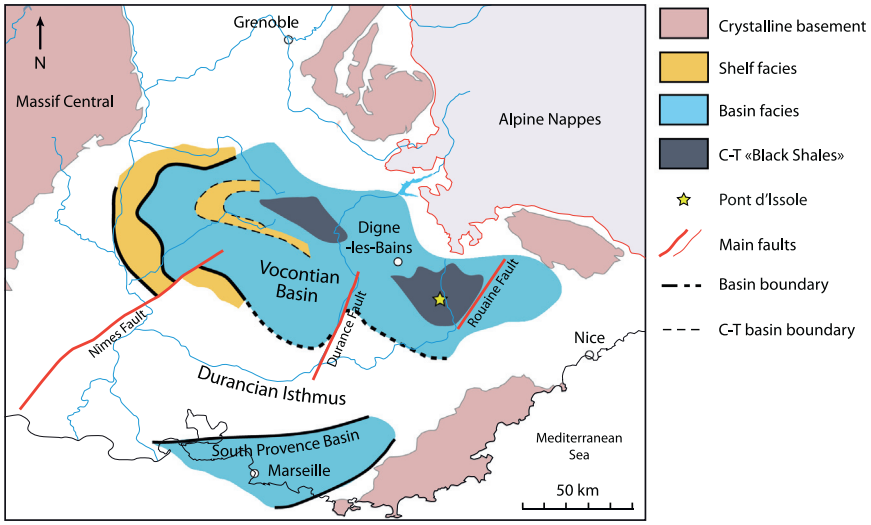

Fig. 2. Paleogeographic map of the Cenomanian in SE France (modified after Grosheny et al., 2017). The thick lines represent the basin boundary during the Cenomanian, the thin dashed lines correspond to shore line during the Cenomanian-Turonian boundary associated to the forced regression regime.

display similar trends with a positive excursion of ~2.5‰ recognized worldwide (e.g. Arthur et al., 1988; Jenkyns et al., 1994; Erbacher et al., 2005; Tsikos et al., 2004; Sageman et al., 2006; Forster et al., 2008; Jarvis et al., 2011; Dickson et al., 2017).

3. The Pont d'Issole section

A CTB reference section for the Vocontian Basin is exposed at the locality of Pont d'Issole (44° 4′11.66″N–6°28′57.56″E) near the village of Thorame-Basse. The Pont d'Issole section is a 26 m outcrop displaying an alternation of marlstones and limestones (Fig. 3) and exposes continuously the Niveau Thomel (~22 m) which is locally defined by the interval between the first apparition of a marly sedimentation and the last thick marl bed at the top. Following the lithostratigraphic divisions described by Jarvis et al. (2011), the Niveau Thomel comprises four well expressed units, called TH1 to TH4 (Fig. 3).

At the base of TH1, a pale gray bioturbated limestone presents high abundance and diversity of planktonic foraminifera, benthic foraminifera, radiolarians and sponge spicules (Jarvis et al., 2011). Unit TH1 (~4.5 m) corresponds to a calcareous dark shale interval interbedded with fine gray marls. Benthic foraminifera disappear, and planktonic foraminifera are rare and smaller, while radiolarians are common (Grosheny et al., 2006). Bioturbations are limited and dominated by *Chondrites* (Jarvis et al., 2011). An increase in the occurrences of carbonated horizons marks the transition between TH1 and TH2. The second unit, TH2, (~4.5 m) is formed by an alternation of highly bioturbated limestone beds and gray marlstones. They are rich in both planktonic and benthic foraminifera, radiolarians, inoceramid fragments and contain sponge spicules, echinoid fragments and shark teeth (Grosheny et al., 2006). The succession TH3-TH4, each one ~6.5 m thick, is similar to the TH1-TH2 in fossil content and facies. Top of TH3 presents the most laminated and organic-rich shales of the whole section. Unit TH4 exposes an alternation of bioturbated limestones and marls. Particularly rich in planktonic foraminifera, TH4 is however quite poor in other organic remains (Grosheny et al., 2006). Conversely to TH2, TH4 exposes two cm-thick dark marly interbeds.

The position of the CTB at Pont d'Issole is based on paleontological data and chemostratigraphic correlation. Based on the distribution of planktonic foraminifera, the Cenomanian-Turonina transition has been defined between the last occurrence of the upper Cenomanian index species *Rotalipora cushmani* at the top of TH2 and the first occurrence of the lower Turonian index species *Helvetoglobotruncana helvetica* at the bottom of TH4 (Grosheny et al., 2006) (Fig. 3). This interval corresponds to the Partial Range Zone of *Whiteinella archaeocretacea* which results in an uncertainty to locate the base of Turonian within TH3. However, a correlation made by Jarvis et al. (2011) using similarities between carbonate carbon stable-isotope time series recorded along both Pont d'Issole section and the English reference section at Eastbourne, where the stratigraphy is well constrained by ammonites, allows to place the CTB within TH3 at 15.19 m (Fig. 3).

4. Materials and methods

For this study, 60 samples were collected along the 22 m representing the Niveau Thomel in the Pont d'Issole section. The multiproxy approach includes the analyses of preserved organic matter by Rock-Eval pyrolysis, sulfur isotope contents, major and trace elements, and iron mineral speciation. Bulk rock samples were powdered to < 60 µm using a ring and puck mill at the Biogeosciences Laboratory of the Université de Bourgogne Franche-Comté in Dijon, France.

4.1. Rock-Eval pyrolysis

Total organic carbon content (wt% TOC) in samples was determined with the Rock-Eval™ 6 at the ISTeP laboratory of the Sorbonne University following the sequential pyrolysis and oxidation treatment (Espitalié et al., 1985a, 1985b, 1986; Behar et al., 2001) on 60 mg of powdered bulk sample aliquots. Reproducibility (1σ) is better than ± 0.05 wt‰ based on duplicates of laboratory standard.

4.2. Sulfur isotopes

Sulfur extractions from sediments were carried out on 39 samples using the method described by Canfield et al. (1986). This method is based on a wet chemical extraction of the sulfides contained in the samples, 39 in this study, by reduction using a hot and acidic chromium solution (1 M $CrCl_2$, 6 N HCl). Pyrite is, therein, largely the main fraction of chromium reducible sulfur in the sediments. The reaction releases H_2S that is subsequently trapped in a 3% $AgNO_3$ solution in the solid form of Ag_2S. Dried and rinsed Ag_2S is then weighted for gravimetric quantification of sample sulfur content. Ag_2S powder (~500 µg) was mixed with an equivalent weight of tungsten trioxide in tin capsules before combustion in a Vario pyro cube (Elementar GmbH™). Sulfur isotope composition ($\delta^{34}S$) was then measured on the SO_2 molecules using an IsoPrime IRMS device at the Biogeosciences Laboratory. International standards (IAEA-S-1, IAEA-S-2, IAEA-S-3) were used

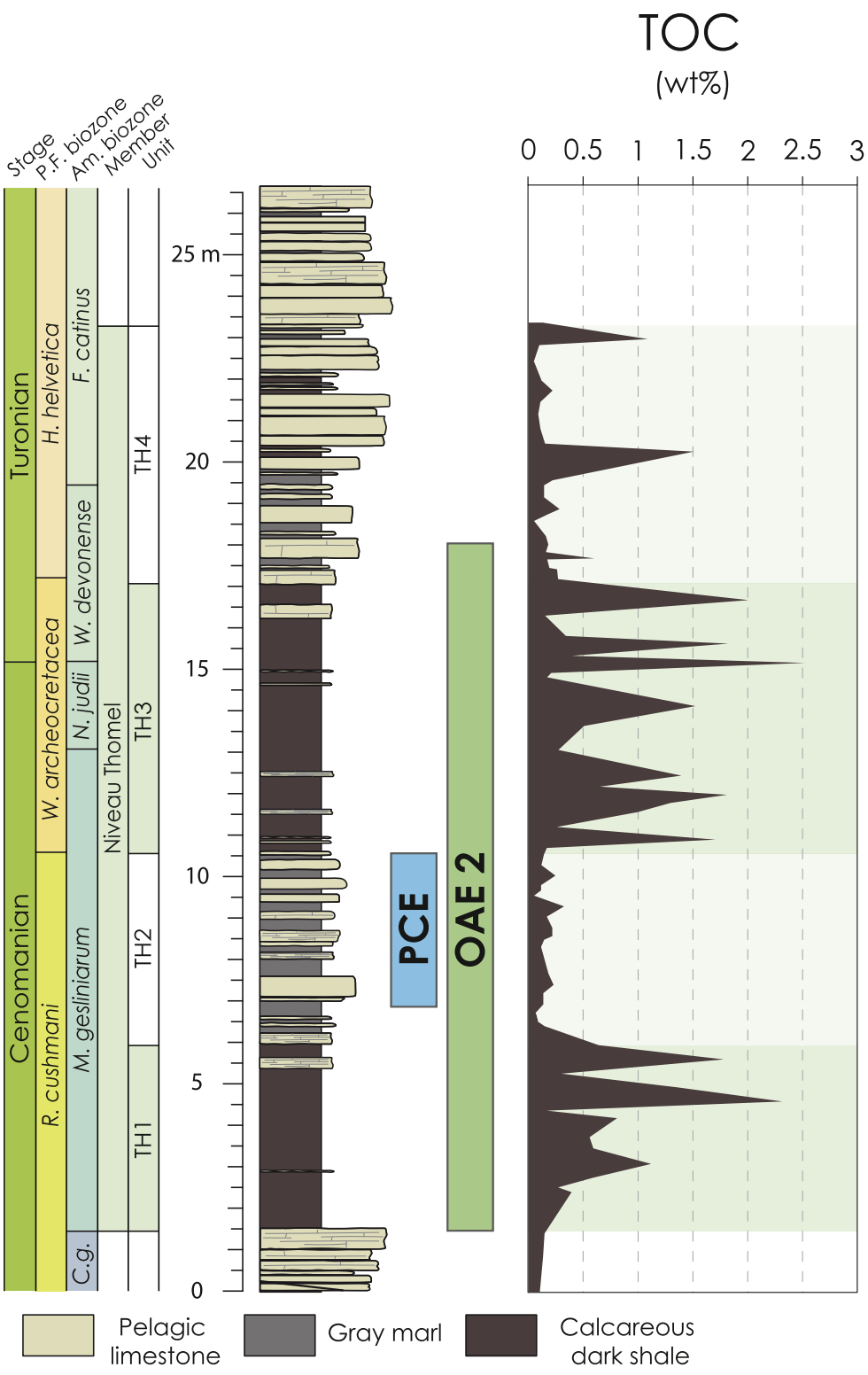

Fig. 3. Total organic carbon and carbon isotopic stratigraphy of the Cenomanian-Turonian boundary along the Pont d'Issole section. Planktonic foraminifera (P.F.) biostratigraphy come from Morel (1998), Grosheny et al. (2006) and Jarvis et al. (2011). Ammonites (Am.) biozones and Cenomanian-Turonian boundary were placed by stratigraphic correlation with Eastbourne section (Jarvis et al., 2011). Greenish bands correspond to the Niveau Thomel units. OAE 2 interval is defined by the interval between the onset of the carbon isotopes excursion and the returning point toward lighter values. Plenus Cold Event (PCE) correspond to the interval marked by a return toward more negative values during the carbon isotope excursion.

for calibration and results were reported in the δ-notation relative to the Vienna Canyon Diablo Troilite (V-CDT) standard. Reproducibility (1σ) is usually better than 0.3‰ based on duplicate analyses.

4.3. Major and trace-element concentration

Selected major (Al, Fe, Mn, P) and trace-element (Mo, U, V, Zn) compositions of 60 samples were determined respectively with an ICP-OES (5100 SVDV Agilent) and an ICP-MS 'QQQ' (8800 Agilent) at the ISTeP laboratory of the Sorbonne University. Acid attacks consisted on simultaneous dissolutions by HF, HNO_3 and HCl for digesting both carbonated and siliciclastic fractions on micropowdered samples. Organic matter was removed by pouring H_2O_2 in the solutions. Standard reference materials and blanks were prepared according to the same procedure. Accuracy and precision of the measures are better than 2% for major elements and 5% for trace elements, determined by international standards and replicate sample analysis.

In order to discriminate major and trace elements from detrital

origin and those representative of the marine background, concentrations have been normalized to Al (e.g. Calvert and Pedersen, 1993; Morford et al., 2001). Al is considered as a robust tracer of detrital input and because of its ability to be not affected by biological or diagenetic processes. Lastly, enrichment factors (EF) with respect to the Upper Crust values (Wedepohl, 1995; Taylor and McLennan, 1985; McLennan, 2001) were calculated following the formula: $EF_{element}\ X = (X/Al)_{sample} / (X/Al)_{Upper\ Crust}$ in order to highlight enrichment from detrital background.

4.4. Iron speciation

Iron mineral speciation and quantification follow the sequential iron extraction procedure proposed by Poulton and Canfield (2005) and described in details in Sauvage et al. (2013). Four different mineral phases were extracted: (1) carbonate-associated Fe (Fe_{carb}) present in siderite and ankerite; (2) Fe contained in oxyhydroxides (Fe_{ox}) including hematite, goethite, akaganeite, lepidocrocite and ferrihydrite; (3) magnetite (Fe_{mag}); (4) Fe bound to poorly reactive sheet silicates (Fe_{PRS}) including biotite, chlorite and glauconite. Each extracted species of iron described above was reacted with phenantroline and the concentration of the resulting Fe^{2+}-phenantroline complex was measured using a Jenways spectral photometer Series 67 at 515 nm, at the Biogeosciences Laboratory, following the method proposed in Reuschel et al. (2012) and described in Sauvage et al. (2013). The concentration of sulfur associated with pyrite (S_{py}) was determined from the chromium reducible sulfur extraction by gravimetric quantification. Iron associated with pyrite (Fe_{py}) was calculated from the S_{py} assuming stoichiometric ratio. Because of their high reactivity toward hydrogen sulfide (Canfield et al., 1992; Poulton et al., 2004), the sum of Fe_{carb}, Fe_{ox}, Fe_{mag} and Fe_{py} are referred as 'Highly Reactive' Fe fraction (Fe_{HR}) of the Fe_T. Fe_{HR}/Fe_T ratio is then commonly used to argue for anoxic conditions when values are above a threshold of 0.38 (Raiswell and Canfield, 1998). Fe_{HR} enrichment, in excess toward this maximal detrital background, indicates an external source of reactive Fe decoupled from the siliciclastic flux. Degree of pyritisation (DOP) corresponding to the ratio of Fe_{py} to total reactive Fe ($Fe_{HR} + Fe_{PRS}$) (Raiswell et al., 1988) is also frequently used as a paleoredox proxy based on empiric thresholds above 0.45 for anoxic conditions and 0.75 for euxinic once.

5. Results

5.1. Organic matter

Variations in TOC along the section agree well with the lithostratigraphic description (Fig. 3). More shaly units within the Niveau Thomel are associated with high TOC values with maximal values within TH1 (TOC = 2.3 wt%) and at the top of TH3 (TOC = 2.5 wt%). Those two intervals are, however, also characterized by variations in TOC within the laminations. Pre-OAE carbonates as well as the carbonated sequences of units TH2 and TH4 are very poor in organic matter, with TOC values mainly lower than < 0.2 wt%. Only two marly interbeds within TH4 show slight TOC enrichment with values of 1.5 and 1.1 wt%, respectively. Those values confirm previous TOC contents found in the Niveau Thomel for this section (Crumière, 1989; Crumière et al., 1991; Crumière et al., 1990; Morel, 1998; Jarvis et al., 2011). As part of the Rock-Eval analyses, the hydrogen and oxygen indices have been obtained and corroborate the previous report of Crumière et al. (1991), arguing for a mixture of Type II and Type III, with a majority of the organic-rich samples associated with Type II.

5.2. Iron mineral speciation

Along the section, the Fe_{HR}/Fe_T values oscillate around the 0.38 threshold representing the boundary between oxic and anoxic conditions (Raiswell and Canfield, 1998) (Fig. 4). In detail, from the base of the section to the top of TH1, Fe_{HR}/Fe_T ratio decrease down to 0.27. Within the TH2, the values are higher and range from 0.26 to 0.58. Within TH3, ratios are close to 0.38 except at the base where it reaches 0.58, and at the top where an extremely elevated Fe_{HR}/Fe_T value (0.84) is recorded. The top of the section, corresponding to TH4, exhibits, relatively lower values and are mostly below the 0.38 canonic threshold.

The DOP signal presents large variations with a strong lithological control. In the two shaly intervals, TH1 and TH3, the DOP shows moderate values, ranging between 0.36 and 0.53. A peak of DOP reaching 0.79 is observed at the top of TH3 and corresponds to the highest value in Fe_{HR}/Fe_T. Transitions from TH1 to TH2, and TH3 to TH4 are characterized by decreasing DOP following the transitions toward more calcareous lithology. Within TH2 and TH4, the low DOP signal is punctually disrupted by few higher values which never exceed 0.37 (Fig. 4).

Like the DOP, S_{py} values are strongly related to the lithological variations with the lowest values recorded in the calcareous intervals (Pre-Thomel, TH2 and TH4) which never exceed 0.2%. Conversely, within TH1 and TH3, S_{py} concentrations are mainly above 0.2%, and the highest S_{py} concentrations correspond to the highest DOP values. It is interesting to note that samples with $S_{py} > 0.2\%$ are concordant with the highest DOP values.

5.3. Sulfur isotopes

TH1 is marked by a rapid ~31.5‰ negative excursion from −8.7‰ at its base to −40.2‰ which is followed by a ~+10‰ increase toward its top. A return toward more negative values (−40.6‰) is observed in TH2. TH3 unit values display a progressive increase in $\delta^{34}S_{py}$ up to a value of −4.9‰ at the TH3–TH4 boundary. TH4 represents a second phase of $\delta^{34}S_{py}$ decrease toward negative values (−34.9‰) up to the top of the Niveau Thomel, which is finally characterized by a return to heavier isotopic compositions (−18.8‰) (Fig. 4).

5.4. Major and trace elements

The EF records for Mo, V and Zn present comparable trends. For most part of the Pont d'Issole section, they show values close to those of Upper Crust element/Al ratio. Only few enrichment peaks are recorded within the shaly intervals at the top of TH1, at the base and at the top of TH3 and within TH4 (Fig. 5). The top of TH1 presents EF for Mo, V and Zn reaching 4.6, 3.0 and 6.0, respectively. The base of TH3 is marked by Mo-enrichments (up to 8.), not seen for V or Zn. Conversely, the top of TH3 is enriched in both Mo (EF = 10.0), V (3.5) and Zn (8.4). Finally, TH4 shaly beds are enriched in V (EF = 2.2 and 2.0, respectively) but not in Mo or Zn (Fig. 5).

Conversely to Mo, V and Zn, uranium does not show a specific enrichment in the shaly intervals of the Niveau Thomel, most of EF U values being close to 1.0.

The EF signal of P exhibits large variations across the Pont d'Issole section. Pre-Thomel samples recorded higher values compared to the Upper Crust (EF > 2.0), but a rapid decline is observed at the Niveau Thomel onset. Thus, TH1 and TH3 present low and stable EF around 0.6. Conversely to the RSTE and TOC contents, enrichments are notable in the carbonated TH2 and TH4 reaching respectively 3.1 and 3.9 (Fig. 6).

Variations of P are broadly correlated with Mn ($r = +0.84$, $p(\alpha) < 0.001$, $n = 60$) and Fe ($r = +0.64$, $p(\alpha) < 0.001$, $n = 60$). Indeed, EF of Fe and Mn exhibit, in the same way as P, large oscillations coeval with lithological changes. For Mn, high contents in pre-Thomel sediments (EF between 1.3 and 2.9) sharply contrast with the very low content recorded within both TH1 and TH3 (EF around 0.3). TH2 and TH4 are marked by high enrichments in comparison to TH1 and TH3 with EF reaching 4.0 and 4.3, respectively. For Fe, most of the EF values roughly correspond to the Upper Crust ratio (EF = 1.0). Fe variations

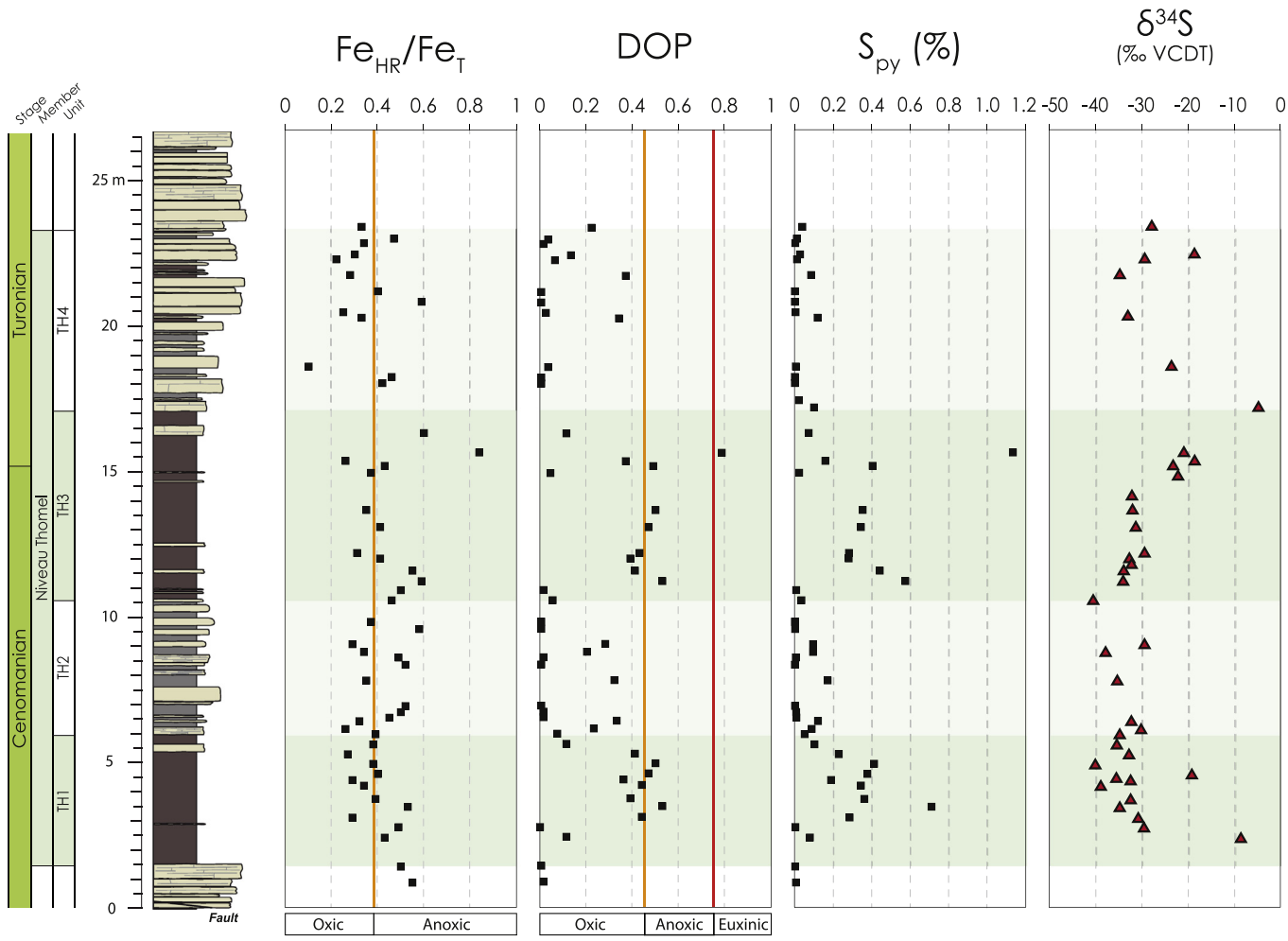

Fig. 4. Mineral iron speciation proxies. Vertical orange line represent thresholds for delimiting oxic and anoxic conditions as described by Raiswell and Canfield (1998) for the Fe_{HR}/Fe_T ratio, and by Raiswell et al. (1988) for the DOP profile. Vertical red line is the threshold for delimiting anoxic and euxinic conditions (Raiswell et al., 1988). Sulfur isotope composition ($\delta^{34}S$) carried out on pyrite.

present lower amplitudes than P and Mn with higher values in TH2 and TH4 (EF = 1.2 and 1.3, respectively) and lower values in TH1 and TH3 (EF = 0.7 and 0.6, respectively).

6. Interpretations

6.1. Iron mineral speciation

Iron speciation measurements (Fe_{HR}/Fe_T and DOP) on marine sediments have been extensively used to approach water column redox conditions in both modern (e.g. Canfield et al., 1996; Raiswell and Canfield, 1998; Poulton and Raiswell, 2002; Lyons and Severmann, 2006) and ancient settings, including OAE sections (März et al., 2008; Westermann et al., 2014; Poulton et al., 2015). Those studies have demonstrated that, under oxic water column conditions, the Fe_{HR}/Fe_T ratio never exceeds a threshold of 0.38 and is commonly found at 0.14 ± 0.08 in ancient sediments (Poulton and Raiswell, 2002). On the contrary, Fe_{HR}/Fe_T values above 0.38 indicate deposition under anoxic conditions.

Along the Pont d'Issole section, the Fe_{HR}/Fe_T signal oscillates around the 0.38 oxic-anoxic threshold. Organic-rich intervals, TH1 and TH3, mostly present moderate values near the threshold. Highest Fe_{HR}/Fe_T recorded in those two intervals are, however, associated with the highest DOP and S_{py} which suggest that variations within TH1 and TH3 are positively correlated with pyrite formation. In the organic-poor intervals, moderate to higher values (between 0.4 and 0.6) are not correlated with high DOP or S_{py} but with the Fe_{ox} and Fe_{carb} fractions (see Supplementary data). This observation indicates that, all along the section, pyrite formation is dependent on the availability of highly-reactive iron. Decrease in Fe_{ox} and Fe_{carb} in the organic-rich intervals suggest an iron reductive zone near the sediment-water interface allowing the liberation of dissolved iron in the water column. High DOP values (> 0.40) and S_{py} concentrations (> 0.2%) coupled with Fe_{HR}/Fe_T ratio close to 0.38 correspond to phases of pyrite formation following high rate of Fe_{ox} and Fe_{carb} dissolution. Episodic phases of concomitant high DOP, S_{py} and Fe_{HR}/Fe_T within TH1 and TH3 suggest that pyrite formation was less iron-limited when MSR zone was better coupled with the iron available in seawater. Beyond this redox-induced iron cycling causing variations in reactive iron availability, changes in siliciclastic input may have also impacted the Fe_{HR}/Fe_T signal (Lyons and Severmann, 2006). Low Fe/Al ratios, under the Upper Crust value (Fig. 6) within the organic-rich intervals suggest higher siliciclastic flux. A dilution by terrigenous supply during these intervals could therefore have contributed to lower the Fe_{HR}/Fe_T. On the contrary, during the carbonate-rich intervals, higher Fe/Al could rather indicate that Fe_{HR} are no longer diluted by the terrigenous flux.

Conversely to the Fe_{HR}/Fe_T, the DOP shows large variations which follow TOC fluctuations along the section. Most of DOP values within organic-rich intervals are located around the 0.45 threshold, suggesting suboxic-anoxic conditions (Fig. 4). As the DOP signal also follows the

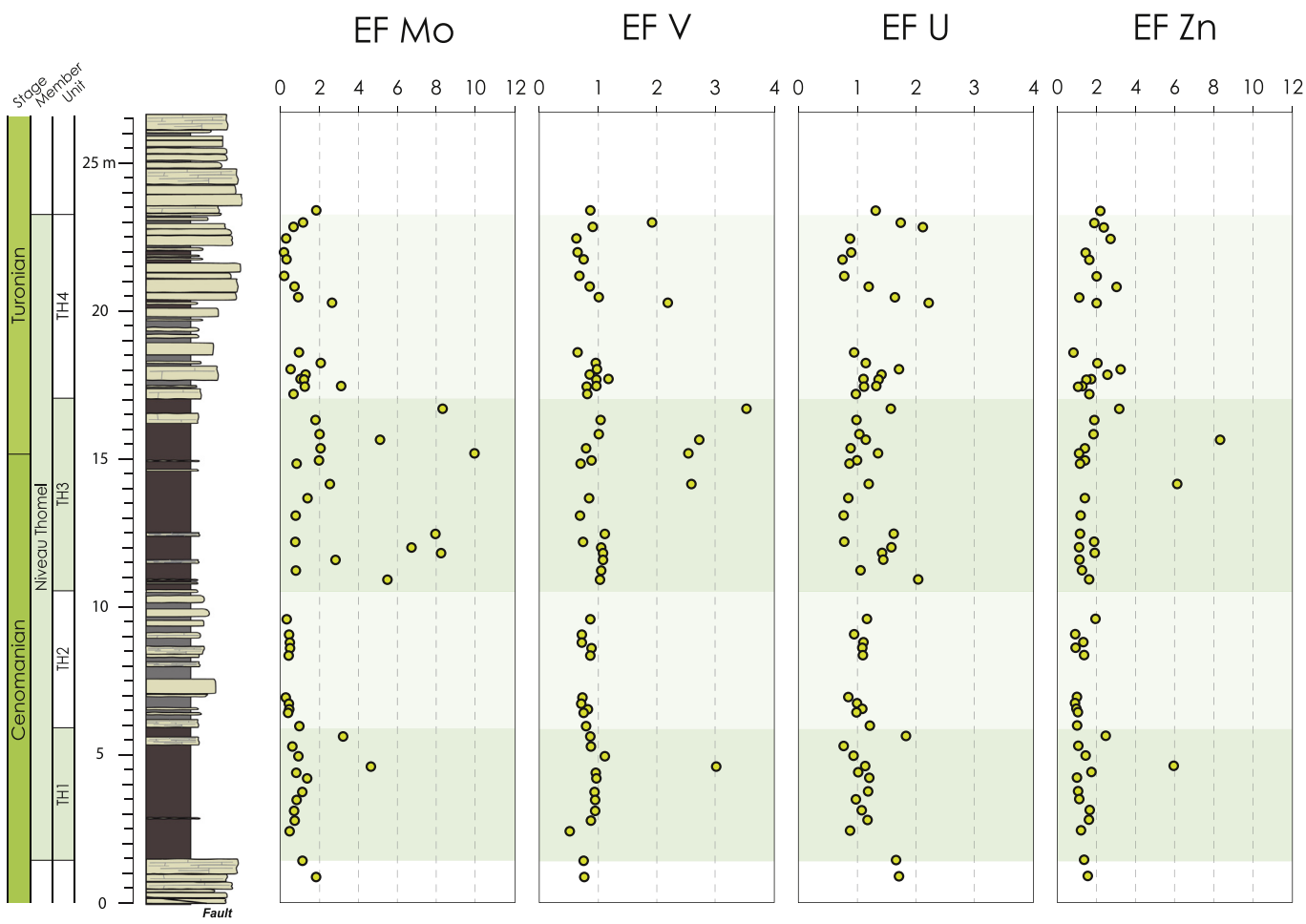

Fig. 5. Enrichment factors (EF) profiles of the redox sensitive trace elements (Mo, V, U, Zn). EF was calculated as $EF(X) = (X / Al)_{sample} / (X / Al)_{Upper\ Crust}$.

concentrations of S_{py}, variations recorded mostly corresponds to the rate of pyrite precipitation, likely reflecting sulfidic pore waters conditions

The evolution of the DOP reflects a rapid transition from oxic to suboxic-anoxic conditions, corresponding to a 0.3 wt% in TOC threshold (Fig. 7) confirming that organic matter is preserved in presence of sulfide in pore waters. Few samples with > 0.3 wt% TOC in the oxic zone in the DOP vs. TOC cross plot are all located at the transition between organic-rich and organic-poor intervals, suggesting a delay between organic-matter preservation in suboxic context and sulfide production by MSR (Fig. 7).

6.2. Redox sensitive elements

The ability of RSTE of being enriched or depleted in the sediments under oxygen-depleted settings has been extensively used for the evaluation of paleo-redox conditions associated with organic-rich deposits (Calvert and Pedersen, 1993; Algeo and Maynard, 2004; Algeo and Lyons, 2006; Brumsack, 2006; Turgeon and Brumsack, 2006; Riquier et al., 2006; Tribovillard et al., 2006). Among them, Mo, U, V and Zn are usually enriched under O_2-depleted conditions and are thus considered to be the most sensitive elements to redox conditions because of their minimal terrigenous influences (Jones and Manning, 1994; Caplan and Bustin, 1999). Others elements as Mn, Fe and P can also be used as redox proxies and could bring complementary information on redox facies. Enrichment factors of these elements was compared to TOC in order to evaluate possible covariations and then for deciphering redox facies (e.g. Algeo and Maynard, 2004).

6.2.1. Molybdenum

Mo uptake from seawater is promoted by Mn-Fe-oxyhydroxides (Calvert and Pedersen, 1993; Crusius et al., 1996; Erickson and Helz, 2000; Zheng et al., 2000) precipitating at the sediment-water interface in well-oxygenated settings. In anoxic bottom waters, Fe-Mn-oxyhydroxides are reduced and Mo is released into solutions as molybdate (MoO_4^{2-}) (Helz et al., 1996; Morse and Luther, 1999; Adelson et al., 2001). Mo can also be accumulated in sediments through adsorption onto humic substances (Brumsack, 1989; Helz et al., 1996). In anoxic sediment pore waters, Mo could be released by sulfate-reducing bacteria decaying this organic matter. Further reduction in presence of hydrogen sulfide leads to the formation of thiomolybdate ($MoO_xS_{(4-x)}^{2-}$, x = 0 to 3; Calvert and Pedersen, 1993). Thiomolybdate is particle-reactive and has the capacity of being scavenged by sulfur-rich organic matter or in iron sulfide (Huerta-Diaz and Morse, 1992; Helz et al., 1996; Tribovillard et al., 2004a). Under O_2-depleted conditions, Mo accumulation is then correlated to H_2S activity (Erickson and Helz, 2000; Zheng et al., 2000). In that case, elevated Mo concentration in sediments rather reflects euxinic conditions than anoxic non-euxinic ones (Algeo and Maynard, 2004; Algeo and Lyons, 2006).

Molybdenum show noticeable enrichment factors (> 4.0) in samples with > 1.5 wt% TOC. These enrichments factors are also concomitant with the highest DOP (> 0.4) and S_{py} values (> 0.2%) suggesting that Mo is likely both present within organic complex and within authigenic sulfides.

6.2.2. Vanadium

V is present in oxic water in the form of vanadate oxyanions

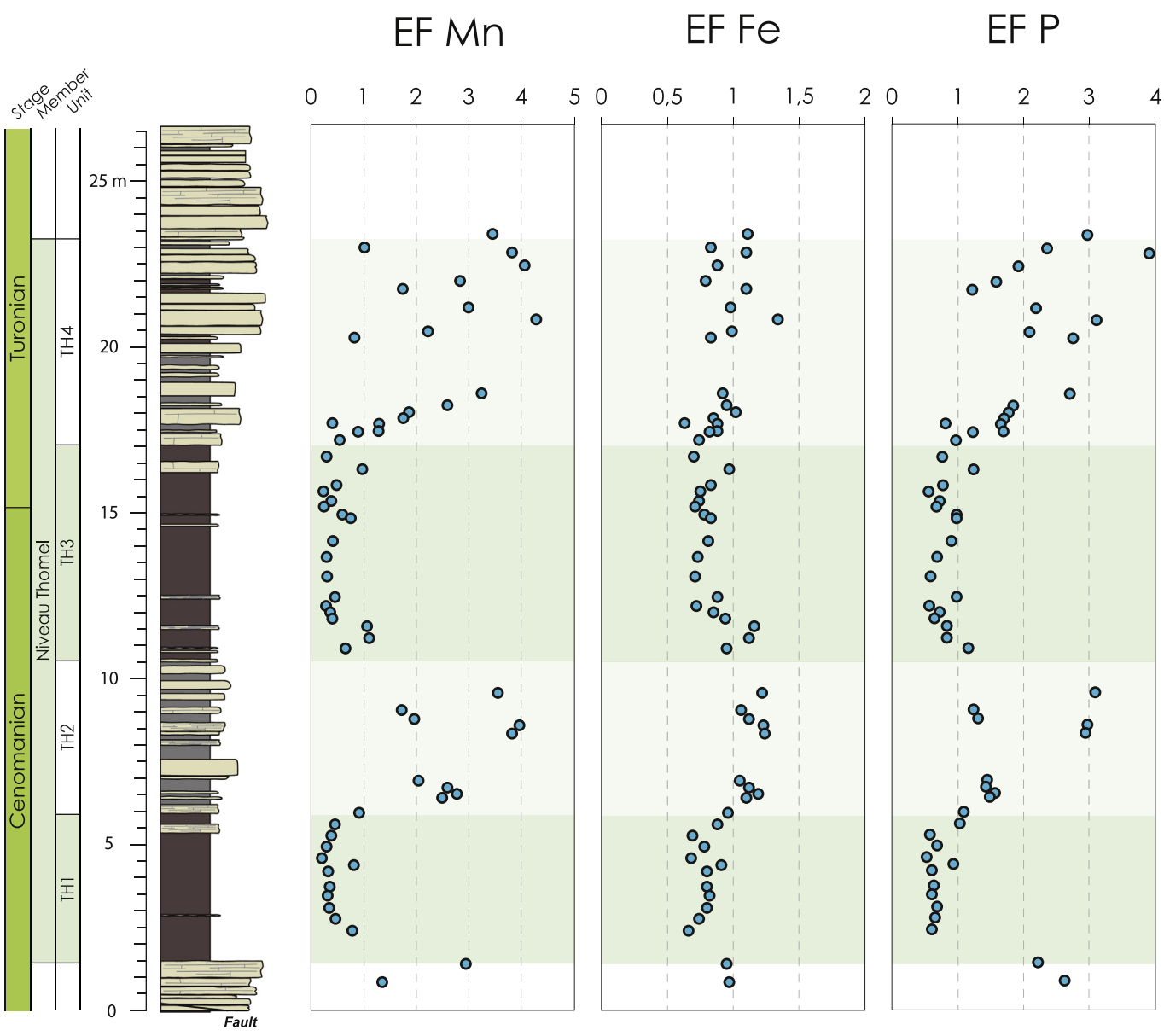

Fig. 6. Enrichment factors (EF) profiles of Mn, Fe and P.

(HVO_4^{2-}) which is mainly adsorbed onto Fe-Mn-oxyhydroxides (Calvert and Piper, 1984). In reducing environments, V is reduced to V (IV) and favors the formation of organometallic ligands (Morford and Emerson, 1999). In the presence of free H_2S, V is reduced into V(III) able to be associated with geoporphyrins or to be precipitated as solid oxide (V_2O_3) or hydroxide ($V(OH)_3$) phase (Breit and Wanty, 1991; Wanty and Goldhaber, 1992). V enrichment in sediments is thus controlled by the degree of anoxia and the formation of these different phases. Under euxinic conditions, V is, conversely to Mo, not scavenged in solid solution by Fe-sulfides but remains in its insoluble oxyhydroxide form.

Vanadium enrichments present two different behaviors above the TOC threshold of 1.5 wt%. A subset of the samples falls on the background concentration trend line while others exhibits a strong positive covariation with TOC followed by an appreciable decrease above 2 wt% TOC (Fig. 8). This dichotomy may be explained by the formation of the two V-bearing phases under anoxic (organometallic ligands) and euxinic conditions (solid oxide and hydroxide) which have contrasted solubilities (Calvert and Pedersen, 1993; Algeo and Maynard, 2004). Low V concentration associated with high TOC is probably due to post-depositional removal from more soluble organometallic ligands. Thus, V enrichments seem to be more indicative of euxinia than Mo.

6.2.3. Zinc

Under oxic environments, Zn acts as a micronutrient and is present as Zn^{2+} or $ZnCl^+$ (Calvert and Pedersen, 1993) but it predominantly forms complexes with humic and fulvic acids (Achterberg et al., 1997) and may also be adsorbed onto particulate Mn-Fe-oxyhydroxides (Fernex et al., 1992). Zn can be enriched in sediments through anoxic conditions, as ZnS, forming a solid solution in pyrite precipitating from MSR activity and in sphalerite ([Zn, Fe]S) (Brumsack, 1980; Huerta-Diaz and Morse, 1992; Morse and Luther, 1999).

Zn content presents, here, noticeable enrichments (up to 3.2) in very low TOC content (< 0.3%) samples probably under conditions where Mn-Fe-oxyhydroxides are stable in the sediments. Zn enrichments also appear in some higher organic-rich samples (TOC > 1.5%) (Fig. 8). Those enrichments are possibly related to the uptake in Fe-sulfides under sulfidic conditions, concordant with the V enrichments.

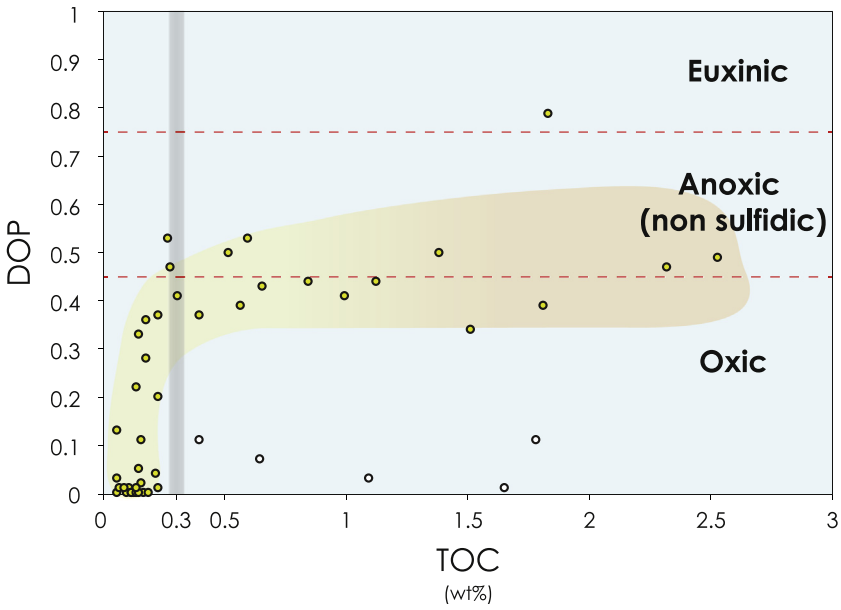

Fig. 7. DOP vs. TOC relationship. Horizontal dashed line corresponds to the limits, defined by Raiswell et al. (1988), between oxic, anoxic and euxinic conditions. Gray shaded limit at 0.3 wt% TOC is the estimated oxic-anoxic threshold. White dots are samples which not follow the general trend by presenting > 0.3 wt% TOC under oxic conditions in the water column. They correspond to the transitional phases between organic-rich and organic-poor intervals when deoxygenated but not sulfate reductive conditions are present in the sediment and with sufficiently rapid organic matter burial.

6.2.4. Uranium

Conversely to Mo, Fe-Mn redox cycling does not influence sedimentary U concentrations. Under oxic conditions, U is present in uranyl carbonate complex form (Calvert and Pedersen, 1993) and its enrichment is limited (Morford et al., 2009). Under anoxic conditions, reduction of U(VI) into U(IV) occurring only within the sediment and formation of highly soluble uranyl ion (UO_2^{+}) allow its uptake with organic-metal ligands on humic acids (Klinkhammer and Palmer, 1991). Increase in uranium in sediment is initiated when Fe(III) becomes reduced into Fe(II) (Zheng et al., 2002). U enrichment occurs, consequently, at weaker reductive conditions than Mo (Morford et al., 2009).

In the Pont d'Issole section, U is enriched neither in the intervals where anoxia was evidenced by mineral iron speciation measurements nor in the > 1.5 wt% TOC samples marked by enrichments of the others RSTE (Fig. 8). This behavior was unexpected because U is prone to be more enriched than Mo in anoxic non-euxinic conditions (Tribovillard et al., 2006; Algeo and Tribovillard, 2009).

However, as it has been demonstrated, U is sensitive to post-depositional reoxygenation to a greater degree than the other RSTE (Morford et al., 2001), then it is highly likely that U was remobilized in the water column because of oxygen penetration within the sediments, via pore fluids circulation.

6.2.5. Manganese and iron

In seawater, Mn(II) is thermodynamically unstable and is oxidized to Mn(III) and Mn(IV) forming oxides (MnO_2) and hydroxides (MnOOH). Reductive dissolution of Mn-oxyhydroxides below the oxic-anoxic interface releases Mn(II) which is not trapped by organic or mineral phases. Mn is then highly recycled under anoxic conditions (Canfield et al., 1993; Algeo and Maynard, 2004). Similar to Fe, Mn redox cycling is very important for trace-element enrichments in sediments because Mn-Fe-oxyhydroxides have the ability to carry several elements, particularly the chalcophile ones (e.g. Zn). These trace elements, released with dissolution of Mn-Fe-oxyhydroxides at or below the water-sediment interface, are then available for scavenging in other phases such as authigenic sulfides. Mn is however not retained in sulfides as iron does.

Reductive dissolution of Mn-Fe-oxyhydroxides is highlighted by exponential decaying from high EF Mn (up to 4.3) in the very poor TOC samples toward low and quite stable values (~0.5) when TOC content exceeds ~0.3% (Fig. 8). Enrichment factors of Fe present the same pathway but amplitude of enrichment is smaller (up to 1.3). The 0.3 wt % TOC is then the threshold above which Mn-Fe-oxyhydroxides formation is strongly limited. This value is also very similar to the oxic-anoxic threshold defined by the DOP vs. TOC (Fig. 7) which suggests that pyrite formation has been promoted by an increase in Fe availability.

6.2.6. Phosphorus

Behavior of phosphorus in the oceans and in sediment is controlled by both organic and inorganic processes. Phosphorus is an essential and often limiting macronutrient for primary productivity (e.g. Tyrrell, 1999) and is thus linked to phytoplankton necromass. Organic matter is then an important source of P in the sediments. Another source of P in sediment can be related to Mn-Fe-oxyhydroxide shuttle (Jarvis et al., 1994; Wang and van Cappellen, 1996; Piper and Perkins, 2004). An additional source of P is the inorganic phosphorus, derived from the sea water (e.g. Föllmi, 1996).

Reactions of degradation of organic matter through aerobic or anaerobic respiration in the water column or in sediments, however, release P as aqueous PO_4^{3-}. This phosphate can also be sorbed onto Mn-Fe-oxyhydroxides in sediments or can precipitated as authigenic P-bearing mineral (e.g. Föllmi, 1996).

Under anoxic conditions, P could diffuse upward in the sediment and return to the water column as regeneration of organic-P become more efficient (Ingall et al., 2005). Released P can return toward the photic zone and enhance primary productivity (e.g. Van Cappellen and Ingall, 1994). As Mn-Fe-oxyhydroxide particles are easily dissolved in reductive conditions, P can also be released from the sediments or either within the water column in case of anoxia developed in bottom waters (e.g. Dellwig et al., 2010). P released through this process reaching the photic zone also enhance primary productivity.

Significant covariation between P and Mn and between P and Fe suggests that P is essentially controlled by the Mn-Fe redox cycling. The evolution of P enrichment shows the same pattern as Mn and Fe regarding the TOC. Depleted P in sediments associated with the highest TOC values also suggest that the P could have also been removed from organic matter. Only two samples display values that do not follow the general exponential decrease. These two samples come from two organic-rich (1.1 and 1.5 wt% TOC, respectively) thin levels within TH4 (Fig. 8). We propose that those P enrichments in TH4 better reflect variations in the magnitude of primary productivity rates compared to fluctuating redox conditions.

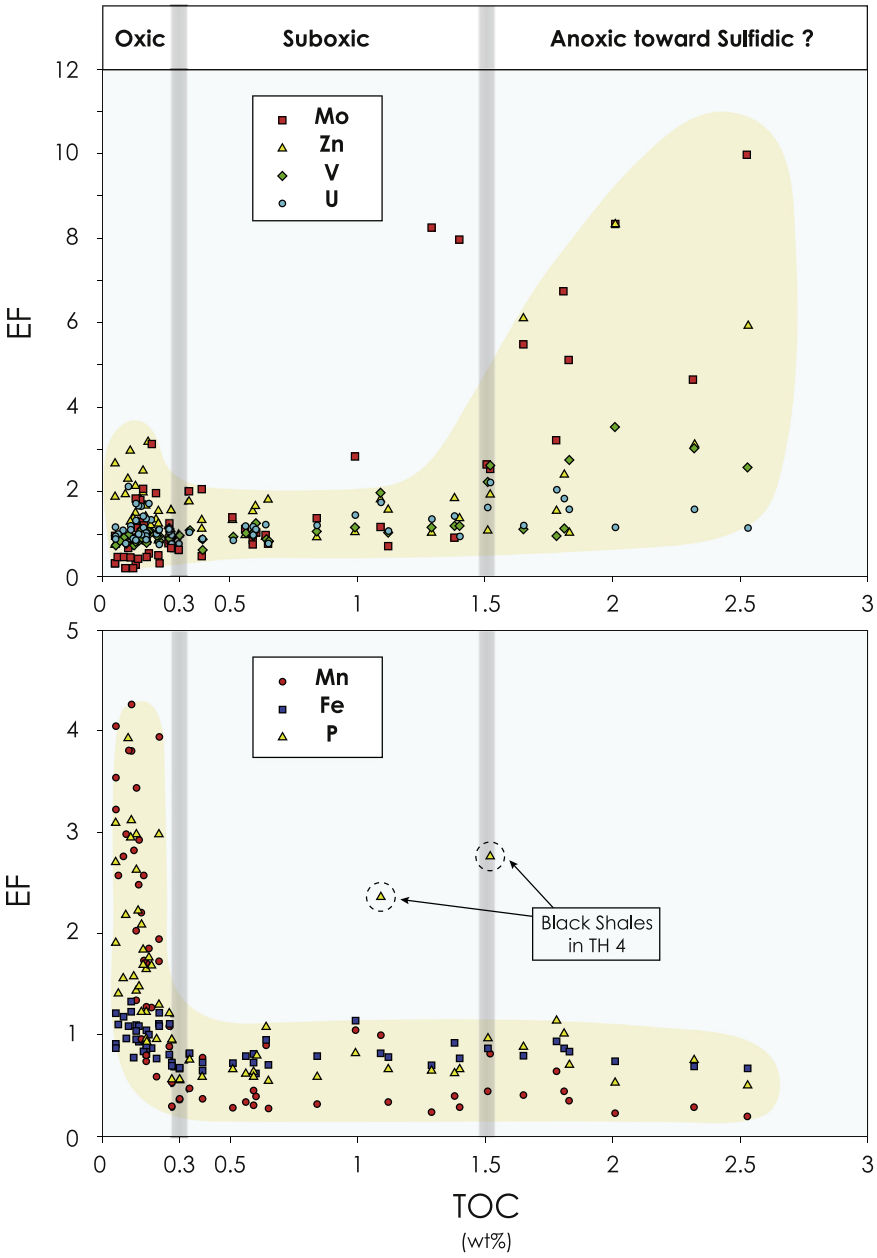

Fig. 8. Enrichments factors of RSTE and Mn, Fe, P confronted to the TOC. The 0.3 wt% TOC threshold defined by the DOP vs. TOC proxy corresponds here to the oxic-suboxic transition on the base of RSTE enrichments. The boundary defined at 1.5 wt% TOC is interpreted as the suboxic-anoxic transition marked by the development of free H_2S toward the sediment-water interface.

6.3. Significance of the elements behavior and evolution of the redox conditions

Trace-element enrichment in sediments is largely attributed to bottom waters deoxygenation because of multiple processes that can lead to trace-elements concentrations, as formation of organometallic ligands, scavenging by Fe-sulfides, formation of authigenic sulfides or oxyhydroxides, are only effective under reducing conditions. However, organic matter accumulation, associated with higher productivity rates, also favors trace-element enrichments in sediments because several of them, serving as bionutrients, are scavenged by organic complexes (Brumsack, 1986). Mo and V enrichments, which reside mainly in authigenic rather than organic phases, are correlated with higher TOC values and with elevated sedimentary pyrite content in the Vocontian Basin, supporting the inference that the driving factor of trace-element enrichment here are O_2-depleted conditions.

Trace-element enrichments vs. TOC has been proved to be a pertinent method to evaluate fine-scale redox variations (e.g. Tribovillard et al., 1994; Algeo and Maynard, 2004; Cruse and Lyons, 2004; Tribovillard et al., 2004b; Tribovillard et al., 2006; Algeo et al., 2007). Sequential enrichments of both trace elements and pyrite in comparison with TOC could allow to discriminate between oxic, suboxic, anoxic non-sulfidic and anoxic sulfidic (euxinic) environments.

Rapid increase of DOP at low TOC underlines an oxic to suboxic-anoxic threshold at ~0.3 wt% TOC (Fig. 7). Above this value, conditions are dominantly anoxic. This threshold is similar to the transition between Mn-Fe-P enriched and depleted sediments. Advective loss of Mn and Fe starts under weakly suboxic conditions (Algeo and Maynard, 2004). Presence of significant bioturbations in < 0.3 wt% TOC samples indicates oxygen concentration of > 0.2 ml $O_2 l^{-1}$ H_2O (Tyson and Pearson, 1991). Enrichments in Mo and Zn under better oxygenated depositional environment (Fig. 8) may also reflect the adsorption onto

Mn-Fe oxyhydroxides (Tribovillard et al., 2006).

Between 0.3 and 1.5 wt% TOC, the EF of Mn, Fe, P remain close to 1 and no noticeable enrichments of Mo, V, Zn and U are recorded (Fig. 8). This interval is then consistent with only manganese and iron reduction at the sediment water interface which mean that the increase in DOP and in S_{py} only records the presence of H_2S and pyrite formation in pore waters. These conditions are referred as suboxic following the definition of Tyson and Pearson (1991).

In samples with > 1.5 wt% TOC, sensible enrichments of Mo, V and Zn are recorded. Preservation of these sulfide-bearing elements underlines anoxic conditions suggesting the presence of free H_2S at least at the water-sediment interface, which is also evidenced by anoxic DOP values.

The interpreted two thresholds at 0.3 wt% TOC and 1.5 wt% TOC, delimiting the three redox facies (oxic, suboxic and anoxic) allow us to propose an evolution of depositional environments and the migration of the redoxcline along the Pont d'Issole section. Establishment of oxygen-depleted conditions at the base of the Niveau Thomel, in the TH1 unit, corresponds to the onset of the OAE 2. Most of the TH1 was deposited under suboxic conditions with some episodic phases of anoxia at the end of the unit, revealing a redoxcline mostly near the sediment-water interface but periodically migrating upward in the bottom waters. A complete reoxygenation of the bottom waters and of the top-part of the sediments during TH2 is concordant with the PCE interval. The end of the PCE marks the return to a phase of oxygen depletion developing all along the TH3 unit. This interval records rhythmically oscillations between suboxic and anoxic conditions, and therein high frequency migration of the redoxcline between the sediment-water interface and the water column. Finally, TH4 represents an ultimate reoxygenation, episodically disrupted by reestablishment of suboxic conditions, concordant with the end of the OAE 2.

7. Discussion

7.1. Record of distant volcanic influences throughout the Niveau Thomel

The hypothesis of a volcanic event triggering the OAE 2 has been extensively investigated because the CTB is coeval with the emplacement of LIPs, like the Caribbean Large Igneous Province (CLIP; Kerr, 1998). A massive magmatic episode would emit important quantities of CO_2 in the atmosphere, leading to a warmer climate and consequently to a decrease in the oxygen solubility in ocean waters (Hotinski et al., 2001). Furthermore, hydrothermal activity associated with LIP emplacements would have brought large amount of reduced metals which would have consumed oceanic O_2 during their oxidation (e.g. Sinton and Duncan, 1997; Snow et al., 2005). Finally, delivery of biolimiting metals (particularly Fe) promoting high primary productivity would further increase heterotrophic O_2 consumption (Sinton and Duncan, 1997).

A global effect of volcanic outgassing on seawater chemistry has been highlighted by osmium-isotope variations across the OAE 2 in many localities all over the world, including Pont d'Issole (Turgeon and Creaser, 2008; Du Vivier et al., 2014, 2015). All localities show a similar Os-isotope profile with an abrupt shift toward unradiogenic values prior to the OAE 2, which supports the hypothesis of the global influence of a volcanic episode(s) triggering this anoxic event (Du Vivier et al., 2014).

At Pont d'Issole, the Os-isotope signal starts to decrease toward unradiogenic values starts just below the Niveau Thomel (Du Vivier et al., 2014; Fig. 9). Values of $^{187}Os/^{188}Os$ remain unradiogenic close to 0.2, up to the TH2-TH3 transition. Then, they are marked by a return to pre-OAE values at the top of the TH3. This implies the occurrence of a volcanic pulse ~40 kyr before the Niveau Thomel onset (Du Vivier et al., 2014). A first pulse associated with a preliminary negative shift is even recognized ~220 kyr before the Niveau Thomel (Du Vivier et al., 2014; Fig. 9). Cessation of volcanic outgassing is estimated at ~200 kyr after the Niveau Thomel first deposit. Those temporal inferences are based on chemostratigraphic correlation with the Portland core (Meyers et al., 2012).

The relationship between volcanic activity and sulfur cycling across the OAE 2 is recently getting attention (Adams et al., 2010; Gomes et al., 2016) because of the temporal correlation between variations in $\delta^{34}S$ and the carbon isotope excursion. The hypothesis of a global change in the biogeochemical sulfur cycling is strengthened by a concordance of a negative excursion in $\delta^{34}S_{py}$ during the carbon isotope excursion in a large range of depositional environments. A negative excursion in $\delta^{34}S_{py}$ during the OAE 2 is found in epicontinental basins such as the Vocontian Basin (this study, Gomes et al., 2016) or the Western Interior Basin (Adams et al., 2010), in open-ocean shelf of the Moroccan margin (Poulton et al., 2015) and in the deep-oceanic setting of the southern North Atlantic (Hetzel et al., 2009).

Low (down to ~−40‰) and invariant $\delta^{34}S_{py}$, as observed within the positive $\delta^{13}C$ excursion along the Pont d'Issole section, reflect a sulfide production under open-system conditions (Lyons, 1997) where the marine sulfate supply is greater than the microbial sulfate reduction rate. In those conditions, the marine sulfate reservoir supply is important enough for sustained sulfate replenishment in the MSR zone and large differences between the isotopic composition of sulfate and sulfide. Additionally, the increase in pyrite burial evidenced by iron mineral speciation results during the OAE 2 at Pont d'Issole supports an expansion of the MSR zone in the sediment toward to sediment-water interface. Enhanced pyrite burial during the OAE 2 in many locations (Hetzel et al., 2009; Adams et al., 2010; Westermann et al., 2014; Poulton et al., 2015; Owens et al., 2017) would then reflect a global shoaling of the MSR zone. In a steady-state system, enhanced pyrite burial should result in an increase in $\delta^{34}S_{py}$ because the burial of pyrite would leave the residual sulfate reservoir, from which it precipitated, enriched in ^{34}S (Fike et al., 2015). Negative $\delta^{34}S_{py}$ excursions associated with the OAE 2 are then controlled by a large-scale transition toward open-system.

This “openness” between sulfate and sulfide reservoirs may have also been enhanced by higher porosity particularly associated with lower sedimentation rate (Pasquier et al., 2017) allowing sulfate diffusion in pore waters. At Pont d'Issole, low $\delta^{34}S_{py}$ is invariant across the transitions between the shaly units and the carbonated unit representing the PCE, which suggest a non-lithologic control. Besides, the onset of the $\delta^{34}S_{py}$ negative excursion is located above the transition between bioturbated carbonates and a laminated shale unit, rather suggesting an evolution toward lower sedimentary porosity. The same $\delta^{34}S_{py}$ evolution in many different settings during the OAE 2, marked by both higher and lower sedimentation rates (Gomes et al., 2016), also argues for non-depositional control. These observations do not support the hypothesis of change in sulfate diffusion through the pore waters due to variations in sedimentation rate or due to change in the lithology.

Previous studies reported that the $\delta^{34}S$ measured on carbonate associated sulfate (CAS), reflecting the isotopic composition of the oceanic sulfate pool, presents an apparent decoupling with the $\delta^{34}S_{py}$ representing the sulfur pool during the OAE 2 (Ohkouchi et al., 1999; Adams et al., 2010; Owens et al., 2013; Poulton et al., 2015; Gomes et al., 2016). The difference between the $\delta^{34}S_{CAS}$ and $\delta^{34}S_{py}$ (generally expressed as $\Delta^{34}S$) is larger with higher sulfate availability (Habicht et al., 2002; Algeo et al., 2015). In the Pont d'Issole section, the apparent decoupling between the isotopic signal of the sulfate (Gomes et al., 2016) and the sulfur reservoir (this study; Fig. 9) then suggest highest sulfate availability at the onset of the Niveau Thomel. Stratigraphically, the correlation between the apparent $\Delta^{34}S$ positive excursion and the Os-isotope excursion at Pont d'Issole (Fig. 9) or at the Portland core (Adams et al., 2010; Du Vivier et al., 2014), suggests a global volcanic-derived sulfate input in the oceans during the OAE 2.

Change in rate of pyrite burial might, however, be reflected in $\delta^{34}S_{CAS}$ variations and, therefore, in the amplitude of fractionation

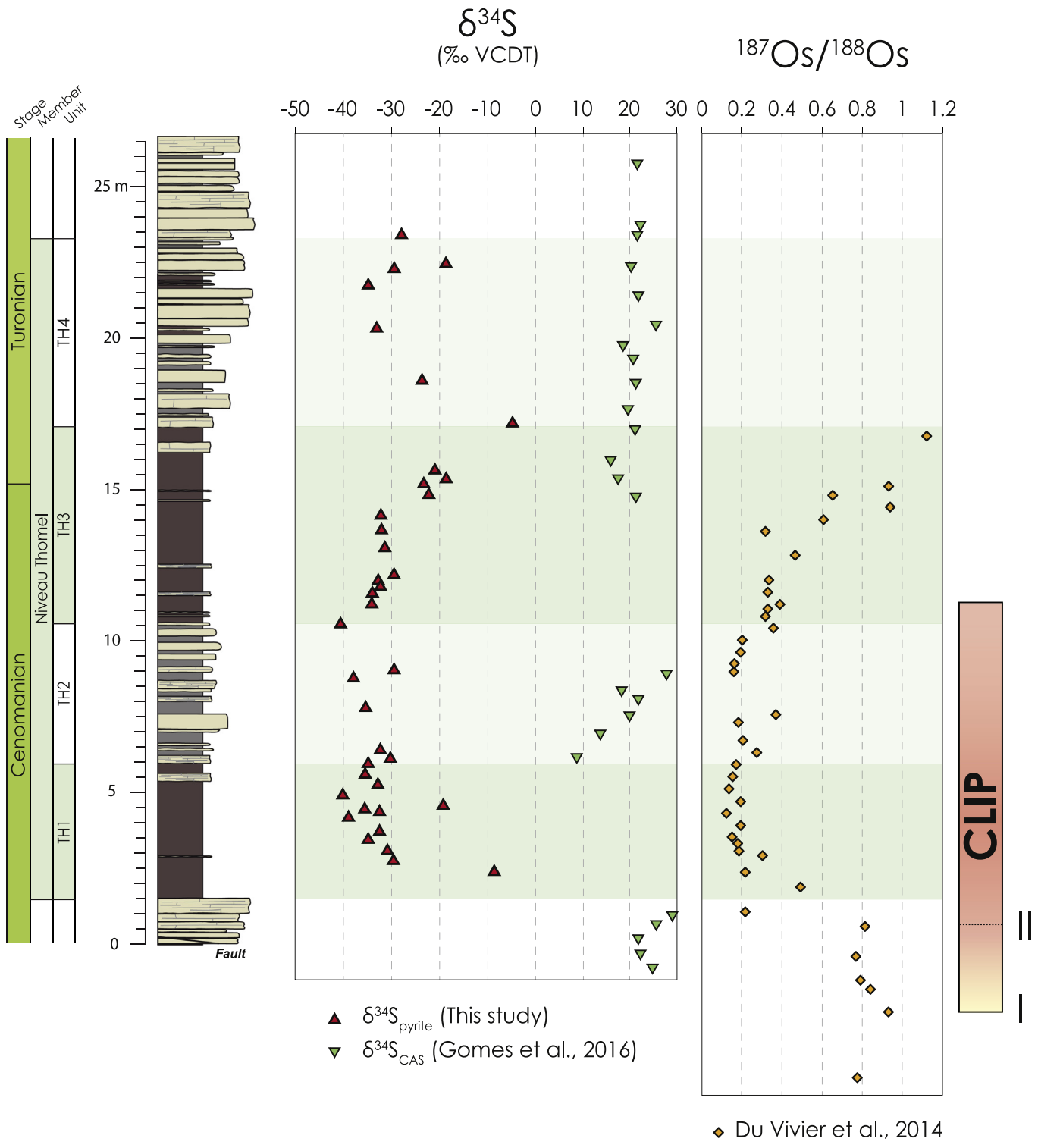

Fig. 9. Sulfur isotope profiles for pyrite (this study) and carbonate-associated sulfate (CAS; Gomes et al., 2016). Os isotope profile along the Pont d'Issole section is from Du Vivier et al. (2014). The onset of CLIP volcanism (I) at ~94.58 Ma, the major pulse (II) at ~94.41 Ma and the cessation at ~94.13 Ma were determined by Meyers et al. (2012) and stratigraphically correlated to the Pont d'Issole section with the carbon isotope excursion (Du Vivier et al., 2014).

between sulfate and sulfide along the Pont d'Issole section. This suggest that sulfate reservoir was limited enough for having its isotopic composition affected by pyrite burial. Return to lower fractionation (i.e. $\Delta^{34}S$) during the organic-rich units would then related to the increase in pyrite burial. The PCE, however, may record a further increase in sulfate availability presumably resulting from a continuous volcanic sulfate input without high rate of pyrite burial. Finally, the termination of the OAE 2 is marked by the return to radiogenic Os values and decreasing $\Delta^{34}S$. We interpret these features here as a reduced influx of sulfate reflecting the progressive cessation of volcanic activity. The concordance of the interpreted global sulfate input in the oceans due to volcanism, related to the Caribbean LIP activity, with the OAE 2 phasing would suggest a cause and effect relationship as proposed by Adams et al. (2010).

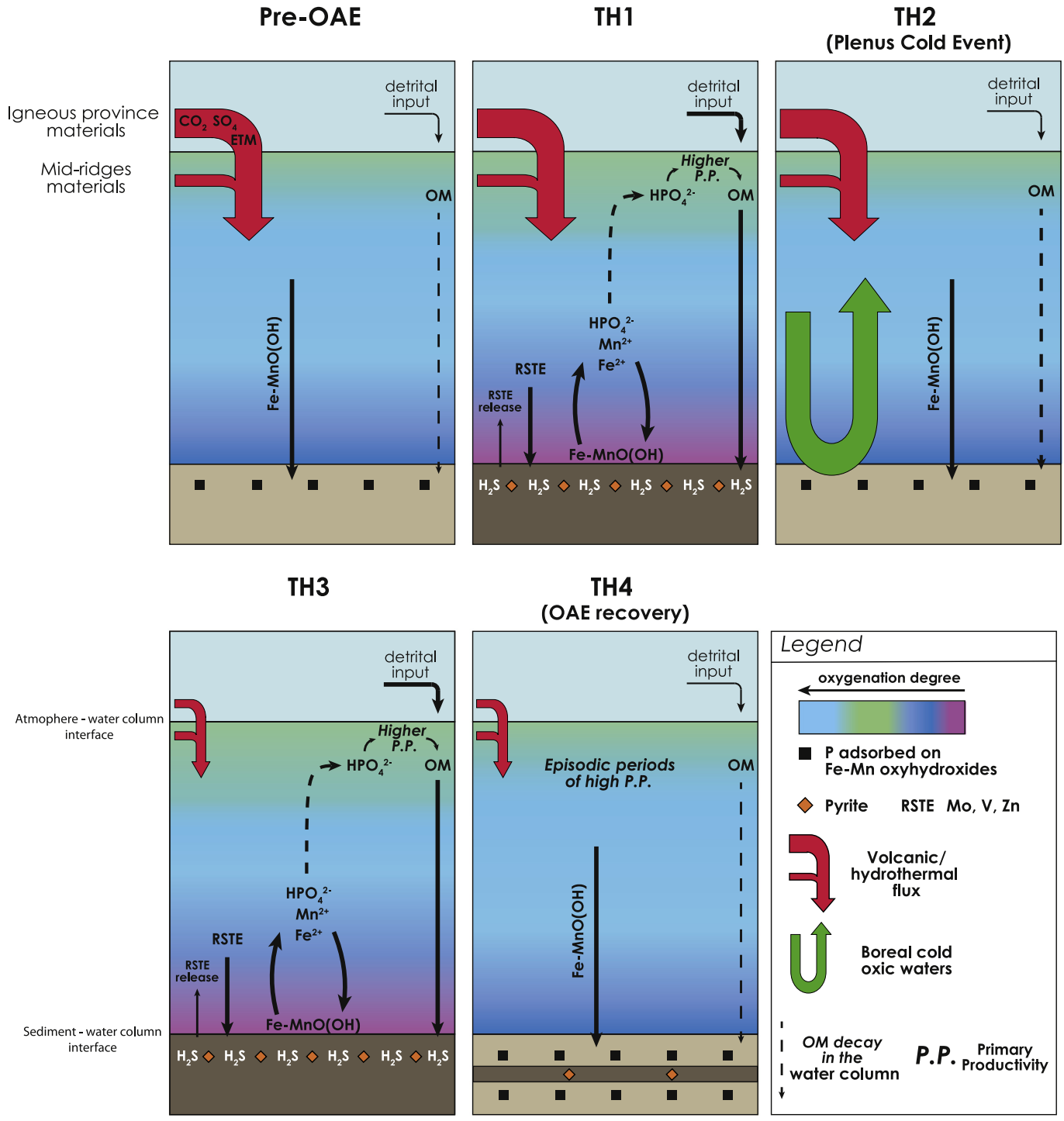

Fig. 10. Schematic representation of the biogeochemical cycles in the water column and in the sediments from the "Pre-OAE" time and through OAE 2 at Pont d'Issole.

7.2. Establishment and expansion of oxygen-depleted conditions during the Niveau Thomel

At Pont d'Issole, episodic RSTE positive anomalies are concordant with the highest TOC samples in the shaly intervals, suggesting only brief deposition under anoxic conditions. These enrichments are quite low, particularly compared to deeper settings in the Western Tethys or Northern Atlantic (e.g. Westermann et al., 2014), and are thus inconsistent with protracted anoxia in the water. Drawdown of trace metals inventory evidenced in deep settings of Northern Atlantic (Hetzel et al., 2009; Goldberg et al., 2016) during the OAE 2 due to basin reservoir effect (Algeo and Rowe, 2012) and development of expanded anoxic to euxinic areas could, however, have limited seawater trace-metal concentrations in the water column of the Vocontian Basin. This mechanism has also been proposed in the Lower Saxony Basin (Hetzel et al., 2011). Besides, in the organic-rich intervals, DOP values (> 0.40) suggests that pore waters experienced phases of larger oxygen depletion. We suggest that the redoxcline has vertically migrated in the upper sediments during these phases and could have reached the bottom waters (Fig. 10). In the intervals with DOP > 0.40, the Fe/Al

ratio shows values below the reference Upper Crust mean value and the Fe_{HR}/Fe_T ratio shows lower values compare to values in the pre-OAE interval or in the PCE. This observation suggests low Fe delivery into the Vocontian Basin during deposition of the Niveau Thomel and an efficient remobilization of the iron oxyhydroxides under suboxic-anoxic conditions. This inference is also supported by the disappearance of Mn in the organic-rich intervals. Conversely to deep settings of Northern Atlantic where euxinic conditions were evidenced on the base of coeval increase in Fe/Al and DOP (Hetzel et al., 2009), the inverse relationship observed at Pont d'Issole suggests that sulfidic conditions were only restricted to the sediment porewaters.

A reactive iron deficiency in the pore waters where MSR is active is consistent with the abrupt increases in DOP revealing an elevated rate of sulfidization of the Fe available within TH1 and TH3. Sedimentary sulfate reduction under Fe-limited conditions may lead to the vulcanization of organic matter (Meyers, 2007; Tribovillard et al., 2015). This process has presumably played an important role in the preservation of organic matter in the Niveau Thomel. Importantly, sulfide production by MSR in the sediments and dissolution of Fe oxyhydroxides, on which P is adsorbed may have in turn promoted P release back into the water column of the Vocontian Basin (Fig.10). Furthermore, replenishment of P in the water column under suboxic conditions is consistent with elevated pyrite burial in the > 0.3 wt% TOC facies.

Enhanced mass accumulation rates of P at the onset of the OAE 2, recorded in deep oceanic basins like the Western Tethys (Mort et al., 2007b) and the Central Atlantic (Hetzel et al., 2009; Kraal et al., 2010; Poulton et al., 2015) or in epicontinental basins (Mort et al., 2007a), have been explained by high primary productivity, possibly linked to a sea level rise, higher weathering rate and volcanic CO_2 input, leading to the expansion of an oxygen minimum zone. In the Wunstorf Basin (Lower Saxony, Germany), where similar TOC values were recorded (up to 2.8 wt%; Hetzel et al., 2011), high primary productivity was evidenced on the base of biomarkers data (Blumenberg and Wiese, 2012). The same interpretation was given by Hetzel et al. (2011) inferred from high P/Al ratio associated with organic-rich intervals. At Pont d'Issole, P is however absent in the organic-rich intervals, while the marine-derived organic matter is mostly well-preserved (Crumière et al., 1991). This feature suggests that productivity is not the primary factor for the organic-matter accumulation. At Pont d'Issole, accumulation of organic matter rather depend to oxygenation conditions in the bottom waters.

Besides, no evidence for P accumulation is observed at the onset of the OAE 2 in the Vocontian Basin, suggesting that primary productivity was not extremely elevated. However, an inverse relation between P and DOP with regard to TOC suggests that sulfide production after MSR during phases of increased sulfate availability have inhibited P burial via Fe-oxyhydroxides. Through this process, release of P within the water column may have contributed to sustain the primary productivity in the photic zone.

A positive feedback relationship between the maintenance of deoxygenated conditions and phosphorus recycling, as proposed by Mort et al. (2007a), is probably relevant for the geochemical record at Pont d'Issole (Fig. 10). The onset of O_2 depletion in sediments with punctual migration of the redoxcline within the water column is presumably the more accurate model explaining an organic matter burial only restricted to the deepest part of the Vocontian Basin.

7.3. An episode of reoxygenated conditions associated with the Plenus Cold Event

Approximately correlated to the TH2 unit in the Pont d'Issole section (Jarvis et al., 2011), the PCE is marked by an absence of RSTE enrichments but is enriched in Mn, Fe and P, indicating Mn-Fe oxyhydroxide burial and oxic bottom waters. The reoxygenation has then been large enough to affect the sediment as well.

In the Pont d'Issole section, the PCE is also characterized by a cessation of organic matter burial, highlighted by extremely low TOC which could be due to a decrease in organic matter production and/or in rapid degradation through the well-oxygenated water column. Under more oxic conditions, P burial with Mn-Fe oxyhydroxides could have led to a decrease in primary productivity. Disruption in organic matter burial, in the Pont d'Issole section, followed a pCO_2 drawdown marked by a drop in the paired inorganic and organic-carbon isotopes ($\Delta^{13}C$) signal before the PCE (Jarvis et al., 2011).

The PCE has been recognized in many outcrops and sites in the northern Hemisphere (e.g. Gale and Christensen, 1996; Forster et al., 2007; Sinninghe Damsté et al., 2010; Jarvis et al., 2011; Zheng et al., 2013) but also in the south Atlantic (Forster et al., 2008) suggesting the existence of a climatic cooling at the global scale, following a massive organic carbon sequestration in sediments in the form of organic matter (Jarvis et al., 2011). This global cooling could have modified ocean circulation as depicted in the Nd isotope record from Eastbourne (Zheng et al., 2013), and ultimately leaded to a migration of oxic and colder boreal water masses into the Vocontian basin, which in turn favored the mixing of the water column.

Moreover, the PCE interval is marked by a positive excursion in the sulfur isotope composition of seawater observed in the Pont d'Issole section (Gomes et al., 2016) as well as in the Eastbourne section (Owens et al., 2013). This positive excursion corresponds to a phase of larger apparent decoupling between sulfur isotope compositions of seawater and pyrite. Following the hypothesis that the difference between the two signals is mainly controlled by sulfate concentration in seawater, the PCE would mark a phase of further increase in sulfate availability during the OAE 2. The most likely reason is that during PCE, a continuous volcanic sulfur outgassing, also suggested by protracted low $^{187}Os/^{188}Os$ values during the OAE 2, was less compensated by sequestration of S in the form of pyrite as indicated by low DOP and S_{py}. We propose that regeneration of both CO_2 and SO_4 seawater concentrations during the PCE could have led to a return to climatic and biogeochemical conditions that have triggered the OAE 2.

8. Conclusions

The sedimentary record of the Niveau Thomel in the Pont d'Issole section offers the opportunity to explore the mechanisms underpinning the redox conditions during the OAE 2 in an epicontinental setting. Variations of redox sensitive elements coupled to mineral iron speciation and organic matter concentration along this section reveal important migrations of the redoxcline between the water column, the sediment-water interface and the sediments through the OAE 2. This study highlights that the depositional environment of the organic-rich intervals were dominated by iron and manganese reduction with brief enrichments in Mo, V and Zn, suggesting an alternation between suboxic and anoxic conditions. A complete reoxygenation of the bottom waters during the Plenus Cold Event interval is in agreement with an incursion of better-ventilated boreal waters into the Vocontian Basin.

Microbially-induced sulfate reduction in sediment pore waters and subsequent sulfide production may have first enhanced the formation of pyrite in a Fe-limited environment. This would have rapidly limited the formation of Fe-oxyhydroxide and then allow the accumulation of H_2S in pore waters which could have reached the sediment-water interface or extended within the bottom waters.

Associated with those oxyhydroxides, P burial has presumably also been limited, promoting its upward diffusion in the water column which could have stimulated the primary productivity and consequently sustaining deoxygenated conditions by exporting organic matter toward the bottom waters.

Large sulfate and carbon dioxide inputs in seawater attributed here to the Caribbean Large Igneous Province outgassing, before the onset of the OAE 2, could have acted as a triggering factor for promoting further oxygen depletion in the Vocontian Basin by enhancing sulfide production and nutrient recycling.

Supplementary data to this article can be found online at https://

doi.org/10.1016/j.chemgeo.2018.05.039.

Acknowledgments

Special thanks to Nicolas Tribovillard and Guillaume Morin for useful discussions that helped for the redaction of this manuscript. We grateful thank Michael E. Böttcher (Chemical Geology editor), Thomas J. Algeo and Karl B. Föllmi for their constructive reviews which greatly improved the quality of the manuscript. We would like to thank Florence Savignac for her analytical assistance for Rock-Eval analysis, Théophile Cocquerez for inorganic isotope measurements, Anne-Lise Santoni and Olivier Mathieu for organic isotope measurements and Benoit Caron for major and trace-element analysis. Iron mineral speciation measurements were, in part, performed by Camille Frau during his master thesis. This study was funded by the project Anox-Sea ANR-12-BS06-0011 coordinated by Emmanuelle Pucéat.

References

Achterberg, E.P., van den Berg, C.M.G., Boussemart, M., Davison, W., 1997. Speciation and cycling of trace metals in Esthwaite water: a productive English lake with seasonal deep-water anoxia. Geochim. Cosmochim. Acta 61, 5233–5253. http://dx.doi.org/10.1016/S0016-7037(97)00316-5.

Adams, D.D., Hurtgen, M.T., Sageman, B.B., 2010. Volcanic triggering of a biogeochemical cascade during Oceanic Anoxic Event 2. Nat. Geosci. 3, 201–204. http://dx.doi.org/10.1038/ngeo743.

Adelson, J.M., Helz, G.R., Miller, C.V., 2001. Reconstructing the rise of recent coastal anoxia; molybdenum in Chesapeake Bay sediments. Geochim. Cosmochim. Acta 65, 237–252. http://dx.doi.org/10.1016/S0016-7037(00)00539-1.

Algeo, T.J., Lyons, T.W., 2006. Mo–total organic carbon covariation in modern anoxic marine environments: implications for analysis of paleoredox and paleohydrographic conditions. Paleoceanography 21, PA1016. http://dx.doi.org/10.1029/2004PA001112.

Algeo, T.J., Maynard, J.B., 2004. Trace-element behavior and redox facies in core shales of Upper Pennsylvanian Kansas-type cyclothems. Chem. Geol. 206, 289–318. http://dx.doi.org/10.1016/j.chemgeo.2003.12.009.

Algeo, T.J., Rowe, H., 2012. Paleoceanographic applications of trace-metal concentration data. Chem. Geol. 324, 6–18. http://dx.doi.org/10.1016/j.chemgeo.2011.09.002.

Algeo, T.J., Tribovillard, N., 2009. Environmental analysis of paleoceanographic systems based on molybdenum–uranium covariation. Chem. Geol. 268, 211–225. http://dx.doi.org/10.1016/j.chemgeo.2009.09.001.

Algeo, T.J., Lyons, T.W., Blakey, R.C., Over, D.J., 2007. Hydrographic conditions of the Devono–Carboniferous North American Seaway inferred from sedimentary Mo–TOC relationships. Palaeogeogr. Palaeoclimatol. Palaeoecol. 256, 204–230. http://dx.doi.org/10.1016/j.palaeo.2007.02.035.

Algeo, T.J., Luo, G.M., Song, H.Y., Lyons, T.W., Canfield, D.E., 2015. Reconstruction of secular variation in seawater sulfate concentrations. Biogeosciences 12, 2131–2151.

Arthur, M.A., Premoli Silva, I., 1982. Development of widespread organic carbon rich strata in the Mediterranean Tethys. In: Schlanger, S.O., Cita, M.B. (Eds.), Nature and Origin of Cretaceous Carbon-rich Facies. Academic, London, pp. 7–54.

Arthur, M.A., Dean, W.E., Pratt, L.M., 1988. Geochemical and climatic effects of increased marine organic carbon burial at the Cenomanian/Turonian boundary. Nature 335, 714–717. http://dx.doi.org/10.1038/335714a0.

Arthur, M.A., Jenkyns, H.C., Brumsack, H.-J., Schlanger, S.O., 1990. Stratigraphy, geochemistry and paleoceanography of organic carbon-rich Cretaceous sequences. In: Ginsburg, R.N., Beaudoin, B. (Eds.), Cretaceous Resources, Events and Rhythms, NATO ASI Ser. C. vol. 301. Kluwer Acad., Dordrecht, Netherlands, pp. 75–119.

Barron, E.J., Fawcett, P.J., Peterson, W.H., Pollard, D., Thompson, S.L., 1995. A "simulation" of mid-Cretaceous climate. Paleoceanography 10, 953–962. http://dx.doi.org/10.1029/95PA01624.

Behar, F., Beaumont, V., De B. Penteado, H.L., 2001. Rock-Eval 6 technology: performances and developments. Oil and gas science and technology. Rev. Inst.t Fr. Pét. 56, 111–134.

Blakey, R., 2011. Global paleogeography. NAU Geology. http://jan.ucc.nau.edu/~rcb7/globaltext2.html.

Blumenberg, M., Wiese, F., 2012. Imbalanced nutrients as triggers for black shale formation in a shallow shelf setting during the OAE 2 (Wunstorf, Germany). Biogeosciences 9, 4139–4153. http://dx.doi.org/10.5194/bg-9-4139-2012.

Breit, G.N., Wanty, R.B., 1991. Vanadium accumulation in carbonaceous rocks: a review of geochemical controls during deposition and diagenesis. Chem. Geol. 91, 83–97. http://dx.doi.org/10.1016/0009-2541(91)90083-4.

Brumsack, H.J., 1980. Geochemistry of Cretaceous black shales from the Atlantic Ocean (DSDP Legs 11, 14, 36, and 41). Chem. Geol. 31, 1–25. http://dx.doi.org/10.1016/0009-2541(80)90064-9.

Brumsack, H.J., 1986. The inorganic geochemistry of Cretaceous black shales (DSDP leg 41) in comparison to modern upwelling sediments from the Gulf of California. In: Summerhayes, C.P., Shackleton, N.J. (Eds.), North Atlantic Palaeoceanography. Geol. Soc. Spec. Publ., vol. 21. pp. 447–462. http://dx.doi.org/10.1144/GSL.SP.1986.021.01.30.

Brumsack, H.J., 1989. Geochemistry of recent TOC-rich sediments from the Gulf of California and the Black Sea. Geol. Rundsch. 78, 851–882. http://dx.doi.org/10.1007/BF01829327.

Brumsack, H.-J., 2006. The trace metal content of recent organic carbon-rich sediments: implications for Cretaceous black shale formation. Palaeogeogr. Palaeoclimatol. Palaeoecol. 232, 344–361. http://dx.doi.org/10.1016/j.palaeo.2005.05.011.

Calvert, S.E., Pedersen, T.F., 1993. Geochemistry of recent oxic and anoxic marine sediments: implications for the geological record. In: Mar. Geol., Marine Sediments, Burial, Pore Water Chemistry, Microbiology and Diagenesis. vol. 113. pp. 67–88. http://dx.doi.org/10.1016/0025-3227(93)90150-T.

Calvert, S.E., Piper, D.Z., 1984. Geochemistry of ferromanganese nodules: multiple diagenetic metal sources in the deep sea. Geochim. Cosmochim. Acta 48, 1913–1928. http://dx.doi.org/10.1016/0016-7037(84)90374-0.

Canfield, D.E., Raiswell, R., Westrich, J.T., Reaves, C.M., Berner, R.A., 1986. The use of chromium reduction in the analysis of reduced inorganic sulfur in sediments and shales. Chem. Geol. 54, 149–155. http://dx.doi.org/10.1016/0009-2541(86)90078-1.

Canfield, D.E., Raiswell, R., Bottrell, S.H., 1992. The reactivity of sedimentary iron minerals toward sulfide. Am. J. Sci. 292, 659–683. http://dx.doi.org/10.2475/ajs.292.9.659.

Canfield, D.E., Thamdrup, B., Hansen, J.W., 1993. The anaerobic degradation of organic matter in Danish coastal sediments: Iron reduction, manganese reduction, and sulfate reduction. Geochim. Cosmochim. Acta 57, 3867–3883. http://dx.doi.org/10.1016/0016-7037(93)90340-3.

Canfield, D.E., Lyons, T.W., Raiswell, R., 1996. A model for iron deposition to euxinic Black Sea sediments. Am. J. Sci. 296, 818–834. http://dx.doi.org/10.2475/ajs.296.7.818.

Caplan, M.L., Bustin, R.M., 1999. Devonian–Carboniferous Hangenberg mass extinction event, widespread organic-rich mudrock and anoxia: causes and consequences. Palaeogeogr. Palaeoclimatol. Palaeoecol. 148, 187–207. http://dx.doi.org/10.1016/S0031-0182(98)00218-1.

Crumière, J.-P., 1989. Crise anoxique à la limite Cenomanien-Turonien dans le bassin subalpin oriental (Sud-Est de la France). Relation avec l'Eustatisme. Geobios 11, 189–203. http://dx.doi.org/10.1016/S0016-6995(89)80056-7.

Crumière, J.P., Crumière-Airaud, C., Espitalié, J., 1990. Préservation cyclique de la matière organique amorphe des sédiments au passage cénomanien-turonien dans le Bassin vocontien (Sud-Est France); contrôles paléo-océanographies. Bull. Soc. géol. Fr. VI 469–478. http://dx.doi.org/10.2113/gssgfbull.VI.3.469.

Crumière, J.P., Crumière-Airaud, C., Schaaf, A., 1991. Les événements de la limite Cénomanien-Turonien dans le domaine subalpin méridional et en Provence. In: Livret-Guide, Grenoble, Mai, (113 pp., unpublished).

Cruse, A.M., Lyons, T.W., 2004. Trace metal records of regional paleoenvironmental variability in Pennsylvanian (Upper Carbonaferous) black shales. Chem. Geol. 206, 319–345.

Crusius, J., Calvert, S., Pedersen, T., Sage, D., 1996. Rhenium and molybdenum enrichments in sediments as indicators of oxic, suboxic, and sulfidic conditions of deposition. Earth Planet. Sci. Lett. 145, 65–78. http://dx.doi.org/10.1016/S0012-821X(96)00204-X.

Dellwig, O., Leipe, T., März, C., Glockzin, Pollehne, F., Schnetger, B., Yakushev, E.V., Böttcher, M.E., Brumsack, H.-J., 2010. A new particulate Mn–Fe–P-shuttle at the redoxcline of anoxic basins. Geochim. Cosmochim. Acta 74, 7100–7115. http://dx.doi.org/10.1016/j.gca.2010.09.017.

Dercourt, J., Ricou, L.-E., Vrielynck, B. (Eds.), 1993. Atlas of Tethys Paleoenvironmental Maps Explanatory Notes. Gauthier-Villars, Paris.

Dickson, A.J., Saker-Clark, M., Jenkyns, H.C., Bottini, C., Erba, E., Russo, F., Gorbanenko, O., Naafs, B.A., Pancost, R.D., Robinson, S.A., van den Boorn, S., Idiz, E., 2017. A Southern Hemisphere record of global trace-metal drawdown and orbital modulation of organic-matter burial across the Cenomanian–Turonian boundary (Ocean Drilling Program Site 1138, Kerguelen Plateau). Sedimentology 64, 186–203. http://dx.doi.org/10.1111/sed.12303.

Donnadieu, Y., Pucéat, E., Moiroud, M., Guillocheau, F., Deconinck, J.F., 2016. A better ventilated ocean triggered by Late Cretaceous changes in continental configuration. Nat. Commun. 7 (10316), 1–12.

Du Vivier, A.D.C., Selby, D., Sageman, B.B., Jarvis, I., Gröcke, D.R., Voigt, S., 2014. Marine $^{187O}s/^{188}Os$ isotope stratigraphy reveals the interaction of volcanism and ocean circulation during Oceanic Anoxic Event 2. Earth Planet. Sci. Lett. 389, 23–33. http://dx.doi.org/10.1016/j.epsl.2013.12.024.

Du Vivier, A.D.C., Selby, D., Condon, D.J., Takashima, R., Nishi, H., 2015. Pacific $^{187}Os/^{188}Os$ isotope chemistry and U–Pb geochronology: synchroneity of global Os isotope change across OAE 2. Earth Planet. Sci. Lett. 428, 204–216. http://dx.doi.org/10.1016/j.epsl.2015.07.020.

Erbacher, J., Friedrich, O., Wilson, P.A., Birch, H., Mutterlose, J., 2005. Stable organic carbon isotope stratigraphy across Oceanic Anoxic Event 2 of Demerara Rise, Western Tropical Atlantic. Geochem. Geophys. Geosyst. 6, Q06010.

Erickson, B.E., Helz, G.R., 2000. Molybdenum(VI) speciation in sulfidic waters. Geochim. Cosmochim. Acta 64, 1149–1158. http://dx.doi.org/10.1016/S0016-7037(99)00423-8.

Espitalié, J., Deroo, G., Marquis, F., 1985a. La pyrolyse Rock-Eval et ses applications, Première partie. Rev. Inst.t Fr. Pét. 40, 563–579.

Espitalié, J., Deroo, G., Marquis, F., 1985b. La pyrolyse Rock-Eval et ses applications, Deuxième partie. Rev. Inst.t Fr. Pét. 40, 755–784.

Espitalié, J., Deroo, G., Marquis, F., 1986. La pyrolyse Rock-Eval et ses applications, Troisième partie. Rev. Inst.t Fr. Pét. 41, 73–89.

Fernex, F., Février, G., Benaïm, J., Arnoux, A., 1992. Copper, lead and zinc trapping in Mediterranean deep-sea sediments: probable coprecipitation with manganese and iron. Chem. Geol. 98, 293–308. http://dx.doi.org/10.1016/0009-2541(92)90190-G.

Fike, D.A., Bradley, A.S., Rose, C.V., 2015. Rethinking the ancient sulfur cycle. Annu. Rev.

Earth Planet. Sci. 43, 593–622.
Föllmi, K.B., 1996. The phosphorus cycle, phosphogenesis and marine phosphate-rich deposits. Earth-Sci. Rev. 40, 55–124. http://dx.doi.org/10.1016/0012-8252(95)00049-6.
Forster, A., Schouten, S., Moriya, K., Wilson, P.A., Sinninghe Damsté, J.S., 2007. Tropical warming and intermittent cooling during the Cenomanian/Turonian oceanic anoxic event 2: sea surface temperature records from the equatorial Atlantic. Paleoceanography 22, PA1219. http://dx.doi.org/10.1029/2006PA001349.
Forster, A., Kuypers, M.M.M., Turgeon, S.C., Brumsack, H.-J., Petrizzo, M.R., SinninghеDamste, J.S., 2008. The Cenomanian/Turonian oceanic anoxic event in the South Atlantic: new insights from a geochemical study of DSDP Site 530A. Palaeogeogr. Palaeoclimatol. Palaeoecol. 267, 256–283. http://dx.doi.org/10.1016/j.palaeo.2008.07.006.
Friedrich, O., Norris, R.D., Erbacher, J., 2012. Evolution of middle to Late Cretaceous oceans-a 55 my record of Earth's temperature and carbon cycle. Geology 40, 107–110. http://dx.doi.org/10.1130/G32701.1.
Frijia, G., Parente, M., 2008. Strontium isotope stratigraphy in the upper Cenomanian shallow-water carbonates of the southern Apennines: short-term perturbations of marine $^{87}Sr/^{86}Sr$ during the oceanic anoxic event 2. Palaeogeogr. Palaeoclimatol. Palaeoecol. 261, 15–29. http://dx.doi.org/10.1016/j.palaeo.2008.01.003.
Gale, A.S., Christensen, W.K., 1996. Occurrence of the belemnite *Actinocamax plenus* in the Cenomanian of SE France and its significance. Bull. Geol. Soc. Den. 43, 68–77.
Goldberg, T., Poulton, S.W., Wagner, T., Kolonic, S.F., Rehkämper, M., 2016. Molybdenum drawdown during Cretaceous Oceanic Anoxic Event 2. Earth Planet. Sci. Lett. 440, 81–91. http://dx.doi.org/10.1016/j.epsl.2016.02.006.
Gomes, M.L., Hurtgen, M.T., Sageman, B.B., 2016. Biogeochemical sulfur cycling during Cretaceous oceanic anoxic events: a comparison of OAE1a and OAE 2. Paleoceanography 31, 2015PA002869. http://dx.doi.org/10.1002/2015PA002869.
Grosheny, D., Beaudoin, B., Morel, L., Desmares, D., 2006. High-resolution biotratigraphy and chemostratigraphy of the Cenomanian/Turonian boundary event in the Vocontian Basin, southeast France. Cretac. Res. 27, 629–640. http://dx.doi.org/10.1016/j.cretres.2006.03.005.
Grosheny, D., Ferry, S., Lécuyer, C., Thomas, A., Desmares, D., 2017. The Cenomanian–Turonian Boundary Event (CTBE) on the southern slope of the Subalpine Basin (SE France) and its bearing on a probable tectonic pulse on a larger scale. Cretac. Res. 72, 39–65. http://dx.doi.org/10.1016/j.cretres.2016.11.009.
Habicht, K.S., Gade, M., Thamdrup, B., Berg, P., Canfield, D.E., 2002. Calibration of sulfate in the Archean ocean. Science 298, 2372–2374. http://dx.doi.org/10.1126/science.1078265.
van Helmond, N.A.G.M., Ruvalcaba Baroni, I., Sluijs, A., Sinninghe Damsté, J.S., Slomp, C.P., 2014. Spatial extent and degree of oxygen depletion in the deep proto-North Atlantic basin during Oceanic Anoxic Event 2. Geochem. Geophys. Geosyst. 15, 4254–4266. http://dx.doi.org/10.1002/2014GC005528.
Helz, G.R., Miller, C.V., Charnock, J.M., Mosselmans, J.L.W., Pattrick, R.A.D., Garner, C.D., Vaughan, D.J., 1996. Mechanisms of molybdenum removal from the sea and its concentration in black shales: EXAFS evidences. Geochim. Cosmochim. Acta 60, 3631–3642. http://dx.doi.org/10.1016/0016-7037(96)00195-0.
Hetzel, A., Böttcher, M.E., Wortmann, U.G., Brumsack, H.-J., 2009. Paleo-redox conditions during OAE 2 reflected in Demerara Rise sediment geochemistry (ODP Leg 207). Palaeogeogr. Palaeoclimatol. Palaeoecol. 273, 302–328. http://dx.doi.org/10.1016/j.palaeo.2008.11.005.
Hetzel, A., März, C., Vogt, C., Brumsack, H.-J., 2011. Geochemical environment of Cenomanian-Turonian black shale deposition at Wunstorf (northern Germany). Cretac. Res. 32, 480–494. http://dx.doi.org/10.1016/j.cretres.2011.03.004.
Hotinski, R.M., Bice, K.L., Kump, L.R., Najjar, R.G., Arthur, M.A., 2001. Ocean stagnation and end-Permian anoxia. Geology 29, 7–10. http://dx.doi.org/10.1130/0091-7613(2001)029<0007:OSAEPA>2.0.CO;2.
Huerta-Diaz, M.A., Morse, J.W., 1992. Pyritization of trace metals in anoxic marine sediments. Geochim. Cosmochim. Acta 56, 2681–2702. http://dx.doi.org/10.1016/0016-7037(92)90353-K.
Ingall, E., Kolowith, L., Lyons, T., Hurtgen, M., 2005. Sediment carbon, nitrogen and phosphorus cycling in an anoxic fjord, Effingham Inlet, British Columbia. Am. J. Sci. 305, 240–258. http://dx.doi.org/10.2475/ajs.305.3.240.
Jarvis, I., Burnett, W.C., Nathan, Y., Almbaydin, F.S.M., Attia, A.K.M., Castro, L.N., Flicoteaux, R., Hilmy, M.E., Husain, V., Qutawnah, A.A., Serjani, A., Zanin, Y.N., 1994. Phosphorite geochemistry—state-of-the-art and environmental concerns. Eclogae Geol. Helv. 87, 643–700.
Jarvis, I., Lignum, J.S., Gröcke, D.R., Jenkyns, H.C., Pearce, M.A., 2011. Black shale deposition, atmospheric CO_2 drawdown, and cooling during the Cenomanian-Turonian Oceanic Anoxic Event. Paleoceanography 26, PA3201. http://dx.doi.org/10.1029/2010PA002081.
Jenkyns, H.C., 1980. Cretaceous anoxic events: from continents to oceans. J. Geol. Soc. Lond. 137, 171–188.
Jenkyns, H.C., 2010. Geochemistry of oceanic anoxic events. Geochem. Geophys. Geosyst. 11, Q03004. http://dx.doi.org/10.1029/2009GC002788.
Jenkyns, H.C., Gale, A.S., Corfield, R.M., 1994. Carbon- and oxygen-isotope stratigraphy of the English Chalk and Italian Scaglia and its palaeoclimatic significance. Geol. Mag. 131, 1. http://dx.doi.org/10.1017/S0016756800010451.
Jones, C.E., Jenkyns, H.C., 2001. Seawater strontium isotopes, oceanic anoxic events, and seafloor hydrothermal activity in the Jurassic and Cretaceous. Am. J. Sci. 301, 112–149. http://dx.doi.org/10.2475/ajs.301.2.112.
Jones, B., Manning, D.A.C., 1994. Comparison of geochemical indices used for the interpretation of palaeoredox conditions in ancient mudstones. Chem. Geol. 111, 111–129. http://dx.doi.org/10.1016/0009-2541(94)90085-X.
Kerr, A.C., 1998. Oceanic plateau formation: a cause of mass extinction and black shale deposition around the Cenomanian–Turonian boundary? J. Geol. Soc. Lond. 155, 619–626. http://dx.doi.org/10.1144/gsjgs.155.4.0619.
Klinkhammer, G.P., Palmer, M.R., 1991. Uranium in the oceans: where it goes and why. Geochim. Cosmochim. Acta 55, 1799–1806. http://dx.doi.org/10.1016/0016-7037(91)90024-Y.
Kraal, P., Slomp, C.P., Forster, A., Kuypers, M.M.M., 2010. Phosphorus cycling from the margin to abyssal depths in the proto-Atlantic during oceanic anoxic event 2. Palaeogeogr. Palaeoclimatol. Palaeoecol. 295 (1), 42–54. http://dx.doi.org/10.1016/j.palaeo.2010.05.014.
Kuroda, J., Ogawa, N.O., Tanimizu, M., Coffin, M.F., Tokuyama, H., Kitazato, H., Ohkouchi, N., 2007. Contemporaneous massive subaerial volcanism and late cretaceous Oceanic Anoxic Event 2. Earth Planet. Sci. Lett. 256, 211–223. http://dx.doi.org/10.1016/j.epsl.2007.01.027.
Leckie, R.M., Bralower, T.J., Cashman, R., 2002. Oceanic anoxic events and plankton evolution: biotic response to tectonic forcing during the mid-Cretaceous. Paleoceanography 17http://dx.doi.org/10.1029/2001PA000623. (13–1).
Lyons, T.W., 1997. Sulfur isotopic trends and pathways of iron sulfide formation in upper Holocene sediments of the anoxic Black Sea. Geochim. Cosmochim. Acta 61, 3367–3382. http://dx.doi.org/10.1016/0016-7037(83)90097-2.
Lyons, T.W., Severmann, S., 2006. A critical look at iron paleoredox proxies: new insights from modern euxinic marine basins. Geochim. Cosmochim. Acta 70, 5698–5722. http://dx.doi.org/10.1016/j.gca.2006.08.021. (A Special Issue Dedicated to Robert A. Berner).
März, C., Poulton, S.W., Beckmann, B., Küster, K., Wagner, T., Kasten, S., 2008. Redox sensitivity of P cycling during marine black shale formation: dynamics of sulfidic and anoxic, non-sulfidic bottom waters. Geochim. Cosmochim. Acta 72, 3703–3717. http://dx.doi.org/10.1016/j.gca.2008.04.025.
McLennan, S.M., 2001. Relationships between the trace-element composition of sedimentary rocks and upper continental crust. Geochem. Geophys. Geosyst. 2, 1021. http://dx.doi.org/10.1029/2000GC000109.
Meyer, K.M., Kump, L.R., 2008. Oceanic euxinia in earth history: causes and consequences. Annu. Rev. Earth Planet. Sci. 36, 251–288. http://dx.doi.org/10.1146/annurev.earth.36.031207.124256.
Meyers, S.R., 2007. Production and preservation of organic matter: the significance of iron. Paeleoceanography 22, PA4211. http://dx.doi.org/10.1029/2006PA001332.
Meyers, S.R., Siewert, S.E., Singer, B.S., Sageman, B.B., Condon, D.J., Obradovich, J.D., Jicha, B.R., Sawyer, D.A., 2012. Intercalibration of radioisotopic and astrochronologic time scales for the Cenomanian–Turonian boundary interval, Western Interior Basin, USA. Geology 40, 7–10. http://dx.doi.org/10.1130/G32261.1.
Monteiro, F.M., Pancost, R.D., Ridgwell, A., Donnadieu, Y., 2012. Nutrients as the dominant control on the spread of anoxia and euxinia across the Cenomanian–Turonian oceanic anoxic event (OAE2): model-data comparison. Paleoceanography 27, PA4209. http://dx.doi.org/10.1029/2012PA002351.
Morel, L., 1998. Stratigraphie à haute résolution du passage Cénomanien-Turonien. Thèse de l'Université Pierre et Marie Curie, Paris VI. (224 pp., unpublished).
Morford, J.L., Emerson, S., 1999. The geochemistry of redox sensitive trace metals in sediments. Geochim. Cosmochim. Acta 63, 1735–1750. http://dx.doi.org/10.1016/S0016-7037(99)00126-X.
Morford, J.L., Russell, A.D., Emerson, S., 2001. Trace metal evidence for changes in the redox environment associated with the transition from terrigenous clay to diatomaceous sediment, Saanich Inlet, BC. Mar. Geol. 174, 355–369. http://dx.doi.org/10.1016/S0025-3227(00)00160-2.
Morford, J.L., Martin, W.R., François, R., Carney, C.M., 2009. A model for uranium, rhenium, and molybdenum diagenesis in marine sediments based on results from coastal locations. Geochim. Cosmochim. Acta 73, 2938–2960. http://dx.doi.org/10.1016/j.gca.2009.02.029.
Morse, J.W., Luther III, G.W., 1999. Chemical influences on trace metal–sulfide interactions in anoxic sediments. Geochim. Cosmochim. Acta 63, 3373–3378. http://dx.doi.org/10.1016/S0016-7037(99)00258-6.
Mort, H.P., Adatte, T., Föllmi, K.B., Keller, G., Steinmann, P., Matera, V., Berner, Z., Stüben, D., 2007a. Phosphorus and the roles of productivity and nutrient recycling during oceanic anoxic event 2. Geology 35, 483–486. http://dx.doi.org/10.1130/G23475A.1.
Mort, H.P., Jaquat, O., Adatte, T., Steinmann, P., Föllmi, K., Matera, V., Berner, Z., Stüben, D., 2007b. The Cenomanian-Turonian anoxic event in Italy and Spain: enhanced productivity and/or better preservation. Cretac. Res. 28, 597–612. http://dx.doi.org/10.1016/j.cretres.2006.09.003.
O'Brien, C.L., Robinson, S.A., Pancost, R.D., Damsté, J.S.S., Schouten, S., Lunt, D.J., Alsenz, H., Bornemann, A., Bottini, C., Brassell, S.C., Farnsworth, A., Forster, A., Huber, B.T., Inglis, G.N., Jenkyns, H.C., Linnert, C., Littler, K., Markwick, P., McAnena, A., Mutterlose, J., Naafs, B.D.A., Püttmann, W., Sluijs, A., van Helmond, N.A.G.M., Vellekoop, J., Wagner, T., Wrobel, N.E., 2017. Cretaceous sea-surface temperature evolution: constraints from TEX86 and planktonic foraminiferal oxygen isotopes. Earth-Sci. Rev. 172, 224–247. http://dx.doi.org/10.1016/j.earscirev.2017.07.012.
Ohkouchi, N., Kawamura, K., Kajiwara, Y., Wada, E., Okada, M., Kanamatsu, T., Taira, A., 1999. Sulfur isotope records around Livello Bonarelli (northern Apennines, Italy) black shale at the Cenomanian-Turonian boundary. Geology 27, 535–538. http://dx.doi.org/10.1130/0091-7613(1999)027<0535:SIRALB>2.3.CO;2.
Owens, J.D., Gill, B.C., Jenkyns, H.C., Bates, S.M., Severmann, S., Kuypers, M.M.M., Woodfine, R.G., Lyons, T.W., 2013. Sulfur isotopes track the global extent and dynamics of euxinia during Cretaceous Oceanic Anoxic Event 2. Proc. Natl. Acad. Sci. U. S. A. 110, 18407–18412. http://dx.doi.org/10.1073/pnas.1305304110.
Owens, J.D., Lyons, T.W., Hardisty, D.S., Lowery, C.M., Lu, Z., Lee, B., Jenkyns, H.C., 2017. Patterns of local and global redox variability during the Cenomanian–Turonian Boundary Event (Oceanic Anoxic Event 2) recorded in carbonates and shales from central Italy. Sedimentology 64, 168–185. http://dx.doi.org/10.1111/sed.12352.

Pasquier, V., Sansjofre, P., Rabineau, M., Revillon, S., Houghton, J., Fike, D.A., 2017. Pyrite sulfur isotopes reveal glacial-interglacial environmental changes. P. Natl. Acad. Sci. USA 114 (23), 5941–5945. http://dx.doi.org/10.1073/pnas.1618245114.
Piper, D.Z., Perkins, R.B., 2004. A modern vs. Permian black shale—the hydrography, primary productivity, and water-column chemistry of deposition. Chem. Geol. 206, 177–197. http://dx.doi.org/10.1016/j.chemgeo.2003.12.006.
Pogge von Strandmann, P.A.E., Jenkyns, H.C., Woodfine, R.G., 2013. Lithium isotope evidence for enhanced weathering during Oceanic Anoxic Event 2. Nat. Geosci. 6, 668–672. http://dx.doi.org/10.1038/ngeo1875.
Porthault, B., 1974. Le Crétacé supérieur de la 'Fosse vocontienne' et des régions limitrophes (France Sud-Est) (Thèse Doct) Etat Université de Lyon Available from: https://tel.archives-ouvertes.fr/.
Poulton, S.W., Canfield, D.E., 2005. Development of a sequential extraction procedure for iron: implications for iron partitioning in continentally derived particulates. Chem. Geol. 214, 209–221. http://dx.doi.org/10.1016/j.chemgeo.2004.09.003.
Poulton, S.W., Raiswell, R., 2002. The low-temperature geochemical cycle of iron: from continental fluxes to marine sediment deposition. Am. J. Sci. 302, 774–805. http://dx.doi.org/10.2475/ajs.302.9.774.
Poulton, S.W., Krom, M.D., Raiswell, R., 2004. A revised scheme for the reactivity of iron (oxyhydr)oxide minerals towards dissolved sulfide. Geochim. Cosmochim. Acta 68, 3703–3715. http://dx.doi.org/10.1016/j.gca.2004.03.012.
Poulton, S.W., Henkel, S., März, C., Urquhart, H., Flögel, S., Kasten, S., Damsté, J.S.S., Wagner, T., 2015. A continental-weathering control on orbitally driven redox-nutrient cycling during Cretaceous Oceanic Anoxic Event 2. Geology 43, 963–966. http://dx.doi.org/10.1130/G36837.1.
Pucéat, E., Lécuyer, C., Sheppard, S.M.F., Dromart, G., Reboulet, S., Grandjean, P., 2003. Thermal evolution of Cretaceous Tethyan marine waters inferred from oxygen isotope composition of fish tooth enamels. Paleoceanography 18, 1029. http://dx.doi.org/10.1029/2002PA000823.
Raiswell, R., Canfield, D.E., 1998. Sources of iron for pyrite formation in marine sediments. Am. J. Sci. 298 (3), 219–245. http://dx.doi.org/10.2475/ajs.298.3.219.
Raiswell, R., Buckley, F., Berner, R.A., Anderson, T.F., 1988. Degree of pyritization of iron as a paleoenvironmental indicator of bottom-water oxygenation. J. Sediment. Res. 58, 812–819. http://dx.doi.org/10.1306/212F8E72-2B24-11D7-8648000102C1865D.
Reuschel, M., Melezhik, V., Strauss, H., 2012. Sulfur isotopic trends and iron speciation from the c. 2.0 Ga Pilgujärvi Sedimentary Formation, NW Russia. Precambrian Res. 196, 193–203. http://dx.doi.org/10.1016/j.precamres.2011.12.009.
Riquier, L., Tribovillard, N., Averbuch, O., Devleeschouwer, X., Riboulleau, A., 2006. The Late Frasnian Kellwasser horizons of the Harz Mountains (Germany): two oxygen-deficient periods resulting from different mechanisms. Chem. Geol. 233, 137–155. http://dx.doi.org/10.1016/j.chemgeo.2006.02.021.
Royer, D.L., Pagani, M., Beerling, D.J., 2012. Geobiological constraints on Earth system sensitivity to CO_2 during the Cretaceous and Cenozoic. Geobiology 10, 298–310. http://dx.doi.org/10.1111/j.1472-4669.2012.00320.
Sageman, B.B., Meyers, S.R., Arthur, M.A., 2006. Orbital time scale and new C-isotope record for Cenomanian–Turonian boundary stratotype. Geology 34, 125–128. http://dx.doi.org/10.1029/2004GC000850.
Sauvage, L., Riquier, L., Thomazo, C., Baudin, F., Martinez, M., 2013. The late Hauterivian Faraoni "Oceanic Anoxic Event" at Río Argos (southern Spain): an assessment on the level of oxygen depletion. Chem. Geol. 340, 77–90. http://dx.doi.org/10.1016/j.chemgeo.2012.12.004.
Schlanger, S.O., Jenkyns, H.C., 1976. Cretaceous oceanic anoxic event: causes and consequences. Geol. Mijnbouw 55, 179–188.
Scholle, P.A., Arthur, M.A., 1980. Carbon isotope fluctuations in Cretaceous pelagic limestones: potential stratigraphic and petroleum exploration tool. AAPG Bull. 64, 67–87.
Sinninghe Damsté, J.S., Kuypers, M.M.M., Pancost, R., Schouten, S., 2008. The carbon isotopic response of algae, (cyano)bacteria, archaea and higher plants to the late Cenomanian perturbation of the global carbon cycle: insights from biomarkers in black shales from the Cape Verde Basin (DSDP Site 367). Org. Geochem. 39, 1703–1718.
Sinninghe Damsté, J.S., van Bentum, E.C., Reichart, G.-J., Pross, J., Schouten, S., 2010. A CO_2 decrease-driven cooling and increased latitudinal temperature gradient during the mid-Cretaceous Oceanic Anoxic Event 2. Earth Planet. Sci. Lett. 293, 97–103. http://dx.doi.org/10.1016/j.epsl.2010.02.027.
Sinton, C.W., Duncan, R.A., 1997. Potential links between ocean plateau volcanism and global ocean anoxia at the Cenomanian-Turonian boundary. Econ. Geol. 92, 836–842. http://dx.doi.org/10.2113/gsecongeo.92.7-8.836.
Snow, L.J., Duncan, R.A., Bralower, T.J., 2005. Trace-element abundances in the Rock Canyon Anticline, Pueblo, Colorado, marine sedimentary section and their relationship to Caribbean plateau construction and oxygen anoxic event 2. Paleoceanography 20, PA3005. http://dx.doi.org/10.1029/2004PA001093.
Takashima, R., Nishi, H., Huber, B., Leckie, R.M., 2006. Greenhouse world and the Mesozoic Ocean. Oceanography 19, 82–92. http://dx.doi.org/10.5670/oceanog.2006.07.
Takashima, R., Nishi, H., Hayashi, K., Okada, H., Kawahata, H., Yamanaka, T., Fernando, A.G., Mampuku, M., 2009. Litho-, bio- and chemostratigraphy across the Cenomanian/Turonian boundary (OAE 2) in the Vocontian Basin of southeastern France. Palaeogeogr. Palaeoclimatol. Palaeoecol. 273, 61–74. http://dx.doi.org/10.1016/j.palaeo.2008.12.001.
Taylor, S.R., McLennan, S.M., 1985. The Continental Crust: Its Composition and Evolution. Blackwell Scientific Publication, Carlton (312 pp.).
Trabucho Alexandre, J., Tuenter, E., Henstra, G.A., van der Zwan, K.J., van de Wal, R.S.W., Dijkstra, H.A., de Boer, P.L., 2010. The mid-Cretaceous North Atlantic nutrient trap: Black shales and OAEs. Paleoceanography 25, PA4201. http://dx.doi.org/10.1029/2010PA001925.
Tribovillard, N.-P., Desprairies, A., Lallier-Vergès, E., Bertrand, P., Moureau, N., Ramdani, A., Ramanampisoa, L., 1994. Geochemical study of organic-matter rich cycles from the Kimmeridge Clay Formation of Yorkshire (UK): productivity versus anoxia. Palaeogeogr. Palaeoclimatol. Palaeoecol. 108, 165–181. http://dx.doi.org/10.1016/0031-0182(94)90028-0.
Tribovillard, N., Riboulleau, A., Lyons, T., Baudin, F., 2004a. Enhanced trapping of molybdenum by sulfurized marine organic matter of marine origin in Mesozoic limestones and shales. Chem. Geol. 213, 385–401. http://dx.doi.org/10.1016/j.chemgeo.2004.08.011.
Tribovillard, N., Trentesaux, A., Ramdani, A., Baudin, F., Riboulleau, A., 2004b. Controls on organic accumulation in late Jurassic shales of northwestern Europe as inferred from trace-metal geochemistry. Bull. Soc. géol. Fr. 491–506. http://dx.doi.org/10.2113/175.5.491.
Tribovillard, N., Algeo, T.J., Lyons, T., Riboulleau, A., 2006. Trace metals as paleoredox and paleoproductivity proxies: an update. Chem. Geol. 232, 12–32. http://dx.doi.org/10.1016/j.chemgeo.2006.02.012.
Tribovillard, N., Hatem, E., Averbuch, O., Barbecot, F., Bout-Roumazeilles, V., Trentesaux, A., 2015. Iron availability as a dominnat control on the primary composition and diagenetic overprint of organic-matter-rich rocks. Chem. Geol. 401, 67–82. http://dx.doi.org/10.1016/j.chemgeo.2015.02.026.
Tsikos, H., Jenkyns, H.C., Walsworth-Bell, B., Petrizzo, M.R., Forster, A., Kolonic, S., Erba, E., Premoli Silva, I., Baas, M., Wagner, T., Sinninghe Damsté, 2004. Carbon-isotope stratigraphy recorded by the Cenomanian-Turonian Oceanic Anoxic Event: correlation and implications based on three key localities. J. Geol. Soc. 161, 711–719. http://dx.doi.org/10.1144/0016-764903-077.
Turgeon, S., Brumsack, H.-J., 2006. Anoxic vs dysoxic events reflected in sediment geochemistry during the Cenomanian–Turonian Boundary Event (Cretaceous) in the Umbria–Marche Basin of central Italy. Chem. Geol. 234, 321–339. http://dx.doi.org/10.1016/j.chemgeo.2006.05.008.
Turgeon, S.C., Creaser, R.A., 2008. Cretaceous oceanic anoxic event 2 triggered by a massive magmatic episode. Nature 454, 323–326. http://dx.doi.org/10.1038/nature07076.
Tyrrell, T., 1999. The relative influences of nitrogen and phosphorus on oceanic primary production. Nature 400, 525–531. http://dx.doi.org/10.1038/22941.
Tyson, R.V., Pearson, T.H., 1991. Modern and ancient continental shelf anoxia: an overview. In: Tyson, R.V., Pearson, T.H. (Eds.), Modern and Ancient Continental Shelf Anoxia. Geol. Soc. Spec. Publ., vol. 58. pp. 1–26. http://dx.doi.org/10.1144/GSL.SP.1991.058.01.01.
Van Cappellen, P., Ingall, E.D., 1994. Benthic phosphorus regeneration, net primary production, and ocean anoxia: a model of the coupled marine biogeochemical cycles of carbon and phosphorus. Paleoceanography 9, 677–692. http://dx.doi.org/10.1029/94PA01455.
Wang, Y., van Cappellen, P., 1996. A multicomponent reactive transport model of early diagenesis: application to redox cycling in coastal marine sediments. Geochim. Cosmochim. Acta 60, 2993–3014. http://dx.doi.org/10.1016/0016-7037(96)00140-8.
Wanty, R.B., Goldhaber, R., 1992. Thermodynamics and kinetics of reactions involving vanadium in natural systems: accumulation of vanadium in sedimentary rock. Geochim. Cosmochim. Acta 56, 171–183. http://dx.doi.org/10.1016/0016-7037(92)90217-7.
Wedepohl, K.H., 1995. The composition of the continental crust. Geochim. Cosmochim. Acta 59, 1217–1232. http://dx.doi.org/10.1016/0016-7037(95)00038-2.
Westermann, S., Vance, D., Cameron, V., Archer, C., Robinson, S.A., 2014. Heterogeneous oxygenation states in the Atlantic and Tethys oceans during Oceanic Anoxic Event 2. Earth Planet. Sci. Lett. 404, 178–189. http://dx.doi.org/10.1016/j.epsl.2014.07.018.
Zheng, Y., Anderson, R.F., van Geen, A., Kuwabara, J., 2000. Authigenic molybdenum formation in marine sediments: a link to pore water sulfide in the Santa Barbara Basin. Geochim. Cosmochim. Acta 64, 4165–4178. http://dx.doi.org/10.1016/S0016-7037(00)00495-6.
Zheng, Y., Anderson, R.F., van Geen, A., Fleisher, M.Q., 2002. Remobilization of authigenic uranium in marine sediments by bioturbation. Geochim. Cosmochim. Acta 66, 1759–1772. http://dx.doi.org/10.1016/S0016-7037(01)00886-9.
Zheng, X.-Y., Jenkyns, H.C., Gale, A.S., Ward, D.J., Henderson, G.M., 2013. Changing ocean circulation and hydrothermal inputs during Ocean Anoxic Event 2 (Cenomanian–Turonian): evidence from Nd-isotopes in the European shelf sea. Earth Planet. Sci. Lett. 375, 338–348. http://dx.doi.org/10.1016/j.epsl.2013.05.053.
Zheng, X.-Y., Jenkyns, H.C., Gale, A.S., Ward, D.J., Henderson, G.M., 2016. A climatic control on reorganization of ocean circulation during the mid-Cenomanian event and Cenomanian-Turonian oceanic anoxic event (OAE 2): Nd isotope evidence. Geology 44, 151–154. http://dx.doi.org/10.1130/G37354.1.